

AN ABSTRACT OF THE THESIS OF

Zachary J. Gonsior for the degree of Master of Science in Geology presented on March 13, 2006.

Title: The Timing and Evolution of Cenozoic Extensional Normal Faulting in the Southern Tobin Range, Pershing County, Nevada.

Abstract approved: _____

John H. Dilles

The Tobin Range of central Nevada lies in the Basin and Range extensional province near the transition between more extended terrane (>50%) to the south and east, and generally less extended terrane to the north and west. Geologic mapping, $^{40}\text{Ar}/^{39}\text{Ar}$ dating and whole-rock geochemical analysis were employed to establish the Cenozoic stratigraphy, geometry and timing of normal faults, and magnitude of extension in the vicinity of Golconda Canyon in the southern Tobin Range.

The Golconda Canyon area lies near the westernmost extent of a major east-west trending paleo-valley that likely predates Basin and Range extension in that region. In-filling and over-topping the paleo-valley are a series of Oligocene to Miocene volcanic rocks. Confined to the paleo-valley is a series of thin basaltic lava flows above which lies the rhyolitic Caetano Tuff (~34 Ma). Units also present in the Golconda Canyon area, but not confined to the paleo-valley include, from bottom to top, a ~700m-thick sequence of andesite lavas, lahars, and ignimbrites (~33 Ma); four

late Oligocene-early Miocene rhyolite ignimbrites; a unit of syn-tectonic landslide breccia and sedimentary rock; and a sequence of fluvial and lacustrine tuffaceous sedimentary rocks intercalated in the center of the section with a 60m-thick series of basaltic lavas (~14 Ma).

Three phases of extensional normal faulting have been identified in the Golconda Canyon area. The earliest phase of normal faulting took place during the early Oligocene in the form of northwest- and northeast-striking, west dipping faults, which resulted in ~20° of tilting in the western part of the Tobin Range and occurred coeval with andesitic volcanism. The next phase of faulting consisted of a major NW striking fault and associated NE striking faults, both of which dip west. These faults moved during the late Oligocene to Middle Miocene and produced syntectonic basins filled with landslide breccia and sedimentary rocks. The last phase of faulting began during the middle Miocene and continues today. This phase of faulting includes north-striking, west-dipping faults localized to the eastern part of the range, where they accommodated ~25° – 30° of tilting. Also present are north-striking faults that dip steeply east. Active faults bound the eastern and western margins of the Tobin Range. The Pleasant Valley fault bounds the western margin of the range, dips to the west, and last ruptured in 1915. The east side of the range is bounded by an east-dipping fault with large displacement in Buffalo Valley but the amount of offset quickly diminishes southward as it enters Jersey Valley. These three phases of normal faulting have resulted in an overall ~25° – 30° eastward tilt of the Tertiary rocks in the Golconda Canyon area. The timing of this faulting and tilting varies, with the western

part of the range being dominated by early Oligocene to early Miocene tectonism, and the eastern part of the range dominated by middle Miocene and younger tectonism.

Palinspastic restorations of cross sections and calculations based on fault and rock unit dips suggest the southern Tobin Range in central Nevada has undergone ~50% east-west crustal extension since 34 Ma. This amount of extension and the initiation of normal faulting at ~33 Ma in the Tobin Range are consistent with the westward decrease in the age and magnitude of extension at this latitude in the Basin and Range Province.

© Copyright by Zachary J. Gonsior

March 13, 2006

All Rights Reserved

The Timing and Evolution of
Cenozoic Extensional Normal Faulting in the
Southern Tobin Range, Pershing County, Nevada.

by

Zachary J. Gonsior

A THESIS

submitted to

Oregon State University

in partial fulfillment of
the requirements for the
degree of

Master of Science

Presented March 13, 2006
Commencement June 2006

Master of Science thesis of Zachary J. Gonsior presented on March 13, 2006

APPROVED:

Major Professor, representing Geology

Chair of the Department of Geosciences

Dean of the Graduate School

I understand that my thesis will become part of the permanent collection of Oregon State University libraries. My signature below authorizes release of my thesis to any reader upon request.

Zachary J. Gonsior, Author

ACKNOWLEDGMENTS

I would like to thank my advisor, John Dilles, as well as my other committee members, Andrew Meigs and Dawn Wright for their helpful input in this research. I would also like to thank John Huard, Bob Duncan, Anita Grunder and Jefferson Hungerford for assistance with mineral separation and Ar/Ar dating analysis, Mark Meyers for computing assistance, and Joe Becker for support in the field. Additional thanks to David John, Chris Henry, and Tom Moore for their feedback and insight on the geology of central Nevada. Lastly, I would like to thank Tia, Joan, James and Rockus Gonsior for their continued support and encouragement.

This research was supported by USGS EdMap grant 05HQPA0004.

TABLE OF CONTENTS

	<u>Page</u>
INTRODUCTION.....	1
Regional Geology.....	2
METHODOLOGY.....	5
Geologic Mapping.....	5
Radiometric Age Determinations.....	5
⁴⁰ Ar/ ³⁹ Ar Results.....	9
STRATIGRAPHY.....	12
Pre-Cenozoic Rocks.....	14
Cenozoic Rocks.....	15
Older Basalts	
Caetano Tuff	
Biotite Rhyolite Ignimbrite	
Andesite	
Late Oligocene Rhyolite Ignimbrites	
Syntectonic Sedimentary Rocks and Breccia	
Younger Rhyolite	
Lacustrine Sedimentary Rocks and Younger Basalt	
Quaternary Deposits	
Rhyolite Geochemistry.....	23
NORMAL FAULTS AND TIMING OF EXTENSION.....	26
Early Oligocene Faults.....	26
Late Oligocene to Middle Miocene Faults.....	28
Middle Miocene and Younger Faults.....	29
DISCUSSION.....	32

Timing and Amount of Extension.....	32
Regional Extension Comparisons.....	34
CONCLUSION.....	36
REFERENCES.....	37
APPENDIX.....	43

LIST OF FIGURES

<u>Figures</u>	<u>Page</u>
1. Shaded relief maps of Nevada showing location of the southern Tobin Range and surface ruptures produced by historic earthquakes in the Central Nevada Seismic Zone.....	2
2. Generalized map showing magnitude of Cenozoic extension in the Basin and Range Province.....	3
3. The geology of Golconda Canyon, southern Tobin Range, Pershing County, Nevada.....	6
4. Cross-sections from the geologic map of Golconda Canyon, southern Tobin Range, Pershing County, Nevada.....	8
5. $^{40}\text{Ar}/^{39}\text{Ar}$ radiometric age plateaus.....	11
6. Range front of the Tobin Range near Golconda Canyon, looking east.....	13
7. Generalized stratigraphic section of Cenozoic rocks in the Golconda Canyon area of the Tobin Range, Nevada.....	16
8. Whole rock geochemistry plots for rhyolite ignimbrite samples.....	24
9. Schematic cross-sections showing a time-sequence of extensional faulting in the Tobin Range.....	27
10. Geologic map showing examples of early Oligocene faults.....	28
11. Geologic map showing example of a steeply east dipping middle Miocene or younger fault.....	30
12. Shaded relief map of Nevada showing the location of estimates of extension.....	35
13. $^{40}\text{Ar}/^{39}\text{Ar}$ age data, A) weighted age plateau, B) K-Ca plateau, C) normal isochron plot, D) inverse isochron plot.....	45

LIST OF TABLES

<u>Tables</u>	<u>Page</u>
1. Summary of $^{40}\text{Ar}/^{39}\text{Ar}$ age data for Cenozoic volcanic rocks.....	10
2. Whole rock geochemistry values	25

LIST OF APPENDIX TABLES

<u>Tables</u>	<u>Page</u>
3. Detection limits for the ICP-MS and x-ray fluorescence methods.....	48
4. Whole rock geochemistry data.....	49

The Timing and Evolution of Cenozoic Extensional Normal Faulting in the Southern Tobin Range, Pershing County, Nevada

INTRODUCTION

Extension and magmatism in the Great Basin began in the late Eocene and have generally migrated southward and westward (Seedorff, 1991). Numerous studies have been conducted to estimate the amount and timing of extension via Cenozoic normal faulting at various locations throughout the Basin and Range Province (i.e. Proffett, 1977; Wernicke et al., 1988; Smith, 1992; Hudson et al., 2000). The southern Tobin Range in Pershing County, Nevada, (Figure 1) is of considerable interest for understanding extensional structural geology because it lies near the apparent transition between more extended terrane (~100%) to the south and east (Proffett, 1977; Smith et al., 1991; Hudson et al., 2000), and generally less extended terrane (~15%) to the north and west (Lerch et al., 2004; Colgan et al., 2006; Figure 2). Despite these different estimates of extension across this apparent boundary, geophysical data suggest that the crust is relatively thin on both sides of the transition (Klemperer et al., 1986). This study was undertaken to map a region in the southern Tobin Range in order to 1) describe the geometry of normal faults, 2) establish the relative and absolute ages of faulting, and 3) estimate the amount of total extension. Geologic mapping, descriptions of volcanic and syntectonic sedimentary deposits, and radiometric dating of volcanic units have been employed to better understand the nature of late Cenozoic normal faulting in the Tobin Range.

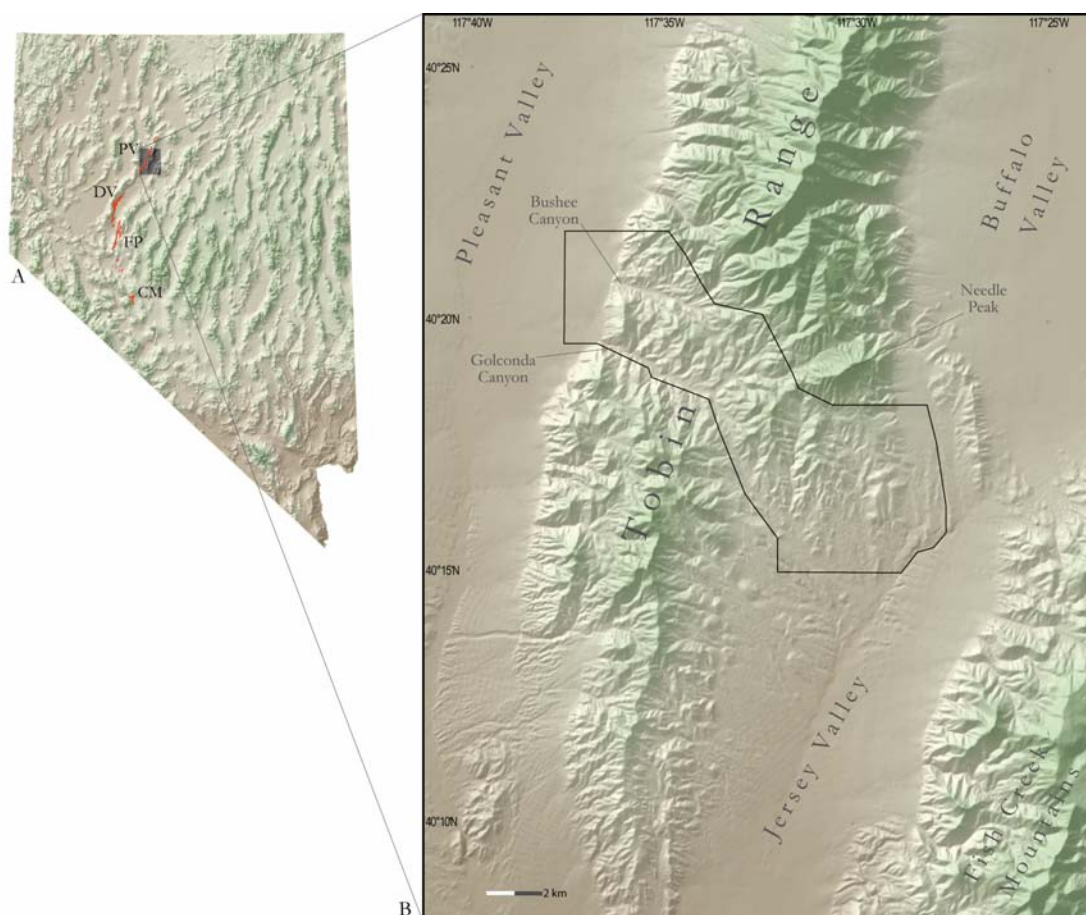


Figure 1. A) Shaded relief maps of Nevada showing location of the southern Tobin Range and surface ruptures produced by historic earthquakes in the Central Nevada Seismic Zone. PV – 1915 Pleasant Valley earthquake, DV – 1954 Dixie Valley earthquake, FP – 1954 Fairview Peak earthquake, CM – 1932 Cedar Mountain earthquake. B) Location of the study area in the Tobin Range.

Regional Geology

The Tobin Range in central Nevada is situated in the actively extending Basin and Range Province. Generally east-west extension via north-striking normal faults in this area has resulted in the development of tilted fault blocks and has generated predominately north-trending mountain ranges separated by alluvial basins. Major characteristics of the Basin and Range Province include high average elevation, high

heat flow, and thin crust (Stewart, 1978). Heat flow in the Province ranges from 60 mW m⁻² in the Eureka low, in central Nevada, to 110 mW m⁻² in the Battle Mountain high in which the Tobin Range is situated (Blackwell et al., 1991). Catchings and Mooney (1991) estimated crustal thicknesses of 32-36 km with the use of seismic reflection profiles at latitude 40° N.

Crustal extension via normal faulting has been associated with intermediate and bimodal mafic-silicic volcanism beginning in the northern part of the Province during the late Eocene, and extension migrated south and west across Nevada

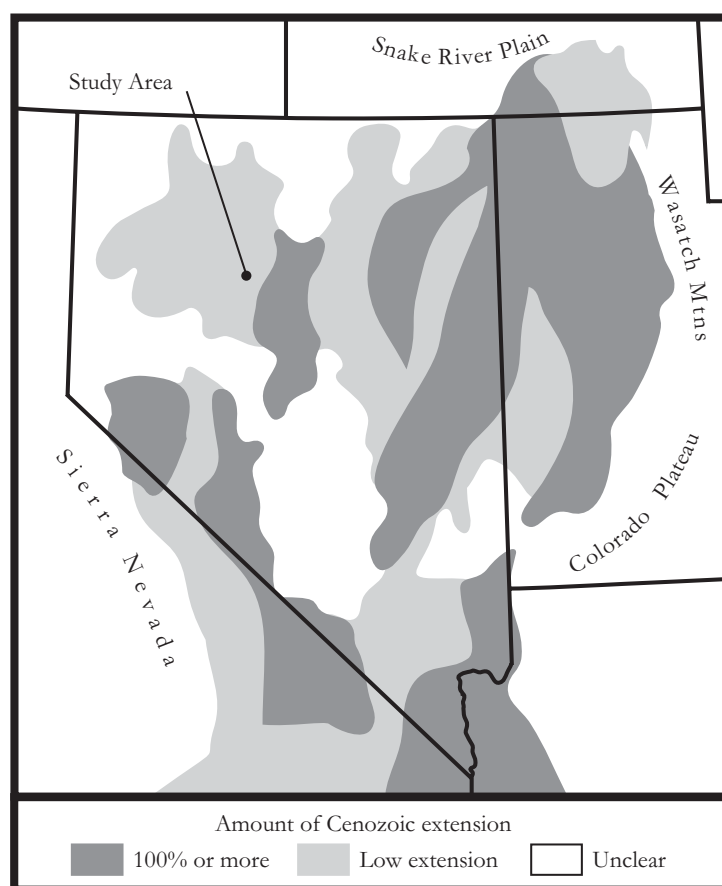


Figure 2. Generalized map showing magnitude of Cenozoic extension in the Basin and Range Province. From E.L. Miller, personal communication (2002).

during the Oligocene and Miocene (e.g. Christiansen and McKee, 1978; Gans et al., 1989; Seedorff et al., 1991; Wernicke, 1992). The elevated heat flow associated with volcanism may have thermally weakened the crust and aided extension in the Basin and Range Province (e.g. Gans et al., 1989). Alternatively, Best and Christiansen (1991) suggested that periods of increased volcanism do not coincide with times of extension. Despite continued faulting and non-homogeneous extension of the upper crust, each part of the Basin and Range Province remains in isostatic equilibrium through ductile flow of the lower crust and upper mantle (e.g. Gans, 1987; Block and Royden, 1990; Wernicke, 1990; McKenzie et al., 2000).

Today, the greatest strain rates in the Basin and Range Province are along the eastern and western margins of the Province (DePolo et al., 1991). Recurrence intervals for faults in the Province are estimated to be several thousands of years to more than 100 thousand years and estimated average slip rates for large, range-bounding faults are between 0.01 to 1.0 mm/yr (Wallace, 1987).

The Tobin Range lies within the Central Nevada Seismic Zone (CNSZ), a seismically active region that has experienced a number of historical earthquakes (Figure 1A). Four large surface-rupturing earthquakes of magnitude > 6.5 have occurred in historical time in the CNSZ. From north to south, they are the 1915 Pleasant Valley earthquake (Wallace, 1984), which ruptured along the western margin of the Tobin Range, the 1954 Dixie Valley and Fairview Peak earthquakes (Slemmons, 1957), and the 1932 Cedar Mountain earthquake (Gianella and Callagan, 1933; Gianella and Callagan, 1936).

METHODOLOGY

Geologic Mapping

Ten weeks of geologic mapping were undertaken during the summers of 2004 and 2005 on portions of the Needle Peak and Jersey Summit 7.5' USGS topographic map quadrangles. Mapping was done at a scale of 1:12,000 on USGS topographic maps and digital orthophotographs and later compiled at a scale of 1:24,000. The resulting geologic map and cross sections can be found on Plate 1 and Figures 3 and 4.

Radiometric Age Determinations

Five samples that showed little alteration were chosen from key areas in the stratigraphy that could help to further constrain the timing of faulting (Table 1). Plate 1 and Figure 3 show the locations where these samples were collected. All samples were cleaned of weathered surfaces, crushed, sieved, and cleaned in de-ionized water and dilute HCl in an ultrasonic bath. Use of a Frantz isodynamic separator, and hand-picking under a binocular microscope, assured 100% purity of mineral separates. Samples TR-9 and TR-81 were plagioclase separates, samples TR05-21 and TR05-26 were sanidine separates and TR-77 was a crushed whole rock sample. A description of the preparation of the mineral separates can be found in the Appendix.

Analytical procedures followed methods described in Duncan and Keller (2004). Samples were wrapped in Cu foil, packed with Fish Canyon Tuff biotite flux monitor standard (28.03 ± 0.18 Ma; Renne et al., 1994) into a sealed silica tube, and

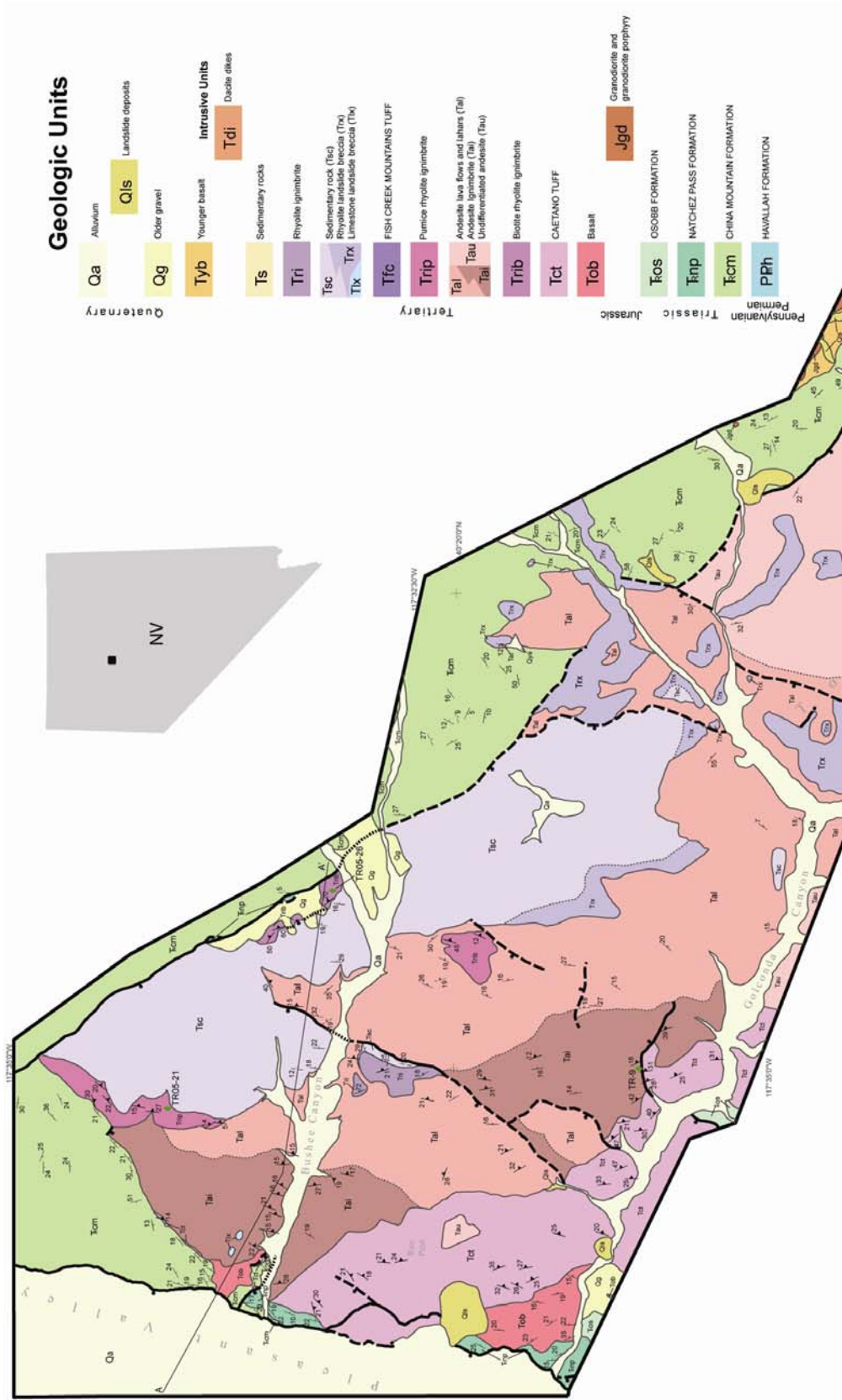


Figure 3. The geology of Golconda Canyon, southern Tobin Range, Pershing County, Nevada

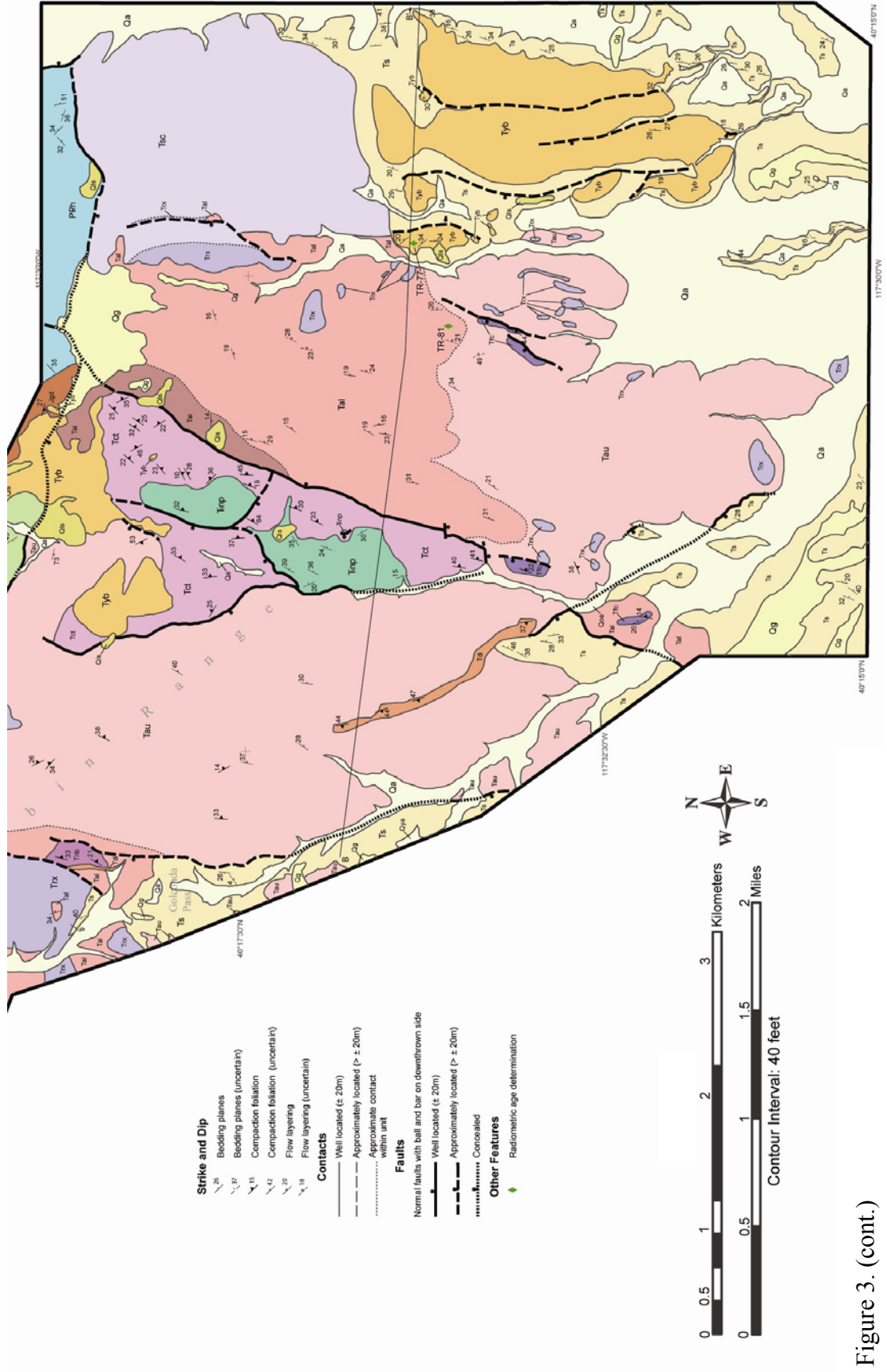


Figure 3. (cont.)

The laser fusion method uses a Merchantek 30 watt CO₂ continuous-fire laser for gas extraction. The laser covers a 50 micron spot on the sample and step-heating of the sample ranges from 400°C to 1500°C. An API Micro Probe model MSP-200G monitors the temperature of the laser. Upon completion of the step-heating, the gas is expanded into the spectrometer for analysis. For both the furnace method and the laser fusion method, contamination is avoided by using a Zr-Al getter between steps and a Zr-V-Fe getter at the end of heating. Software from Koppers (2002) was used to reduce data and determine isotopic ratios, from which the age is calculated using the known age of the flux monitor, 28.03 ± 0.18 Ma (Renne et al., 1994).

The following criteria developed by Dalrymple and Lanphere (1974), Duncan et al. (1997), Tegner and Duncan (1999), and Frey et al. (2004) were used to determine viable closure ages: 1) a plateau is established with a minimum of three contiguous heating steps within the limits of a 2σ error, and represents $\geq 50\%$ of total ³⁹Ar released (the steps are used to calculate the weighted mean plateau age); 2) a mean square of weighted deviates (MSWD) analysis of the weighted mean plateau age is more than 1 but less than 2.5; 3) the plateau age is concordant with the isochron age and; 4) the initial ⁴⁰Ar/³⁶Ar ratio calculated from the isochron is within a 2σ error limit of the ⁴⁰Ar/³⁶Ar ratio for atmospheric argon.

⁴⁰Ar/³⁹Ar Results

Of the five samples submitted for analysis, four met the aforementioned criteria. Sample TR-81 however, did not develop an age plateau but rather a U-shaped pattern of argon release indicating excess argon. Table 1 summarizes the age dates

produced from the analysis. Age plateaus of the samples are shown in Figure 5. The appendix contains additional data and a description of sample preparation. The data are available on the enclosed CD.

Table 1. Summary of $^{40}\text{Ar}/^{39}\text{Ar}$ age data for Cenozoic volcanic rocks. All ages calculated from age plateaus.

Sample	Unit	Rock Type and Stratigraphic Location	Material ¹	^{39}Ar (%), N ²	Age (Ma)
TR05-26	Trib	Rhyolite ignimbrite below andesite sequence	San	95.6, 10/12	33.28 ± 0.22
TR-9	Tai	Ignimbrite near base of andesite sequence	Plag	100, 10/10	33.03 ± 0.25
TR-81	Tal	Lava flow near top of andesite sequence	Plag	71.7, na	No plateau
TR05-21	Trip	Rhyolite ignimbrite below landslide breccia	San	100, 12/14	24.95 ± 0.17
TR-77	Tyb	Near middle of Miocene basalt sequence	w.r.	82.4, 7/10	14.10 ± 0.12

¹plag - plagioclase, san - sanidine, w.r. - whole rock, ²number of heating steps within plateau / total number of heating steps.

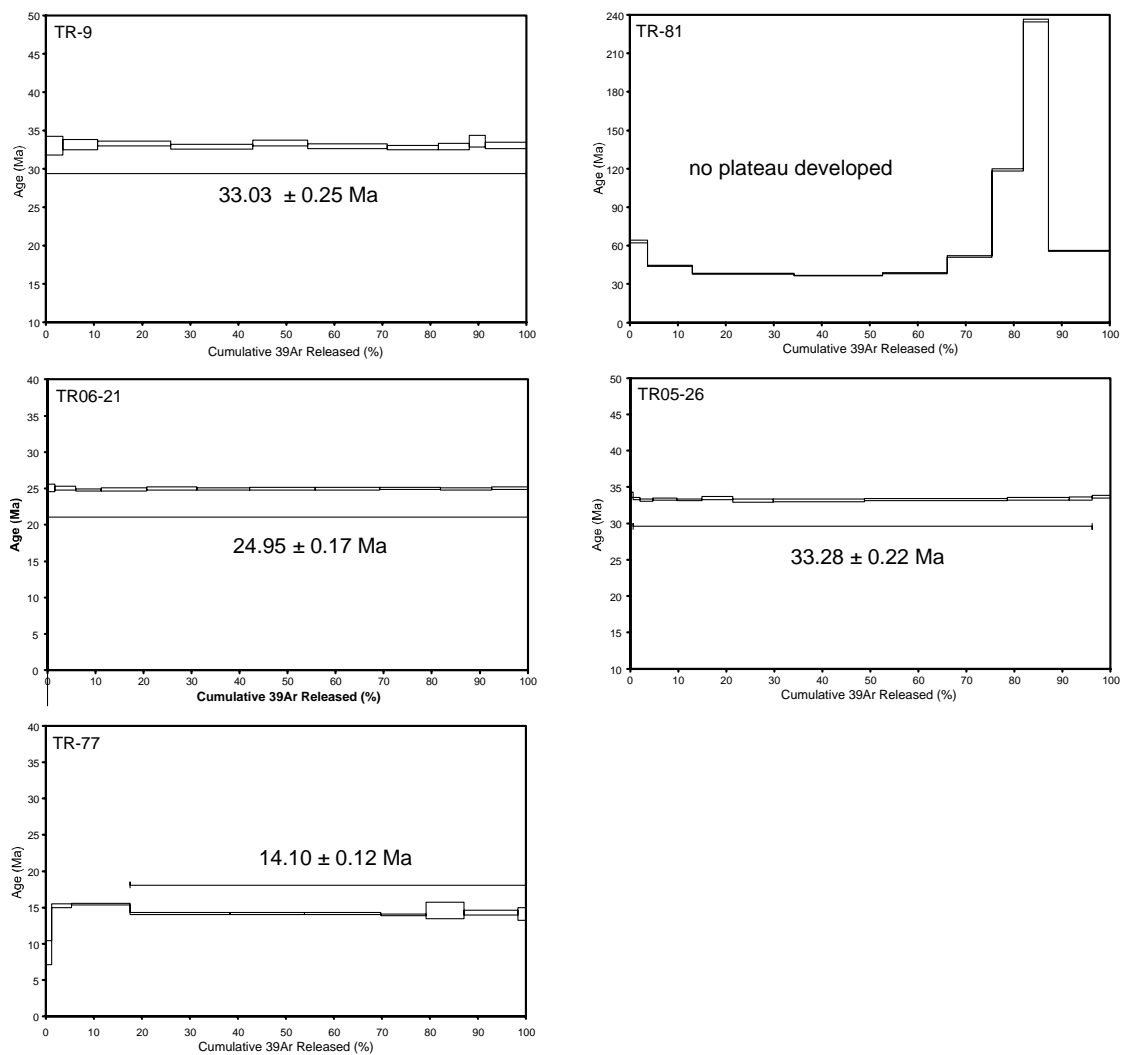


Figure 5. $^{40}\text{Ar}/^{39}\text{Ar}$ radiometric age plateaus.

STRATIGRAPHY

The Golconda Canyon area of the southern Tobin Range consists of a pre-Tertiary east-west trending paleo-valley in-filled, and overtopped, by Tertiary volcanic and sedimentary units (Figure 6). Masursky (1960) and Burke and McKee (1979) originally described this paleo-valley as a volcano-tectonic trough that developed during the Eocene and extended until the Miocene. However, in the Tobin Range, Tertiary units appear unconformably banked into the pre-Tertiary units and the presence of gravels between the Tertiary and pre-Tertiary units near the mouth of Golconda Canyon suggest that the genesis of this feature is erosional, and not tectonic. Other paleo-valleys similar in age and orientation have been documented in west-central Nevada (Proffett and Proffett, 1976; Henry et al., 2003). The northern margin of the Golconda Canyon paleo-valley in the Tobin Range is locally bound by a NW striking normal fault whereas the southern extent of the paleo-valley is less well defined. The width of the paleo-valley is approximately 6-7 km based on the distribution of the Caetano Tuff, a unit that appears to be confined by the paleo-valley.



Figure 6. Range front of the Tobin Range near Golconda Canyon, looking east. Uplift along the range front fault has exposed a “cross-section” of the paleo-valley. Pre-Tertiary units were eroded to form a paleo-valley which was later in-filled by Tertiary volcanic and sedimentary rocks. The Oligocene basalt and Caetano Tuff are restricted to the paleo-valley, whereas andesite and younger units extend south of the valley. Fault scarp, drawn in blue, is from the 1915 Pleasant Valley earthquake.

Pre-Cenozoic Rocks

The oldest rocks in the study area belong to the Pennsylvanian/Permian Havallah Formation, a thick sequence of quartzite, chert, argillite, limestone and rare greenstone (Muller et al., 1951; Ferguson et al., 1952). Also in the vicinity, but not in the map area, is the Pennsylvanian/Permian Pumpnickel Formation, a thick sequence of greenstone, chert and argillite that underlies the Havallah Formation (Muller et al., 1951). These rock units crop out along the northern edge of the field area, in the vicinity of Needle Peak, and underlie much of the central Tobin Range to the north.

The lower-Triassic Koipato Group overlies the Havallah Sequence and consists of four units: the Limerick Greenstone (oldest), the Rochester Rhyolite, the Weaver Rhyolite and the China Mountain Formation (youngest). In the Golconda Canyon area, tuffaceous sandstone, rhyolite- and chert-pebble conglomerate and lesser amounts of rhyolite assigned to the China Mountain Formation are the principal rocks exposed. The age of the Koipato Group is 225 ± 30 Ma on the basis of a fission-track age on zircons from Rochester Rhyolite samples collected in Pleasant Valley (McKee and Burke, 1972).

A granodiorite of unknown age intrudes the Havallah Formation and Koipato Group. On the Pershing County geologic map (Tatlock et al., 1977) this small intrusion is interpreted to be Jurassic in age, similar to several other Jurassic granodiorite intrusions in central Nevada (McKee et al., 1971). Permian, Cretaceous and Tertiary granodiorites have also been identified in Pershing County (Tatlock et al., 1977), thus the Tobin granodiorite may not be Jurassic.

The Natchez Pass Formation of the middle and upper Triassic Star Peak Group, and the Osobb Formation of the upper Triassic Auld Lang Syne Group overlie the Koipato Group. The Natchez Pass Formation is composed of dark gray to brown massive limestone and dolomite, whereas the Osobb Formation is predominantly sandstone. Burke (1973) provides detailed descriptions of the pre-Tertiary stratigraphy in the southern Tobin Range south of Golconda Canyon.

Cenozoic Rocks

Older Basalts

A thick sequence of ignimbrites, lava flows and sedimentary rocks unconformably overlie the pre-Cenozoic rocks. The lowest units, the Oligocene basalts and Caetano Tuff, are confined to the Eocene paleo-valley described above (Figure 6). Figure 7 illustrates the stratigraphic section and relationships of the Cenozoic rock units in schematic form. The oldest unit filling the paleo-valley is a series of up to 25 basalt lava flows comprising a section up to 200 m thick. The basalt has only been observed at the bottom of the paleo-valley near the mouths of Golconda and Bushee Canyon.

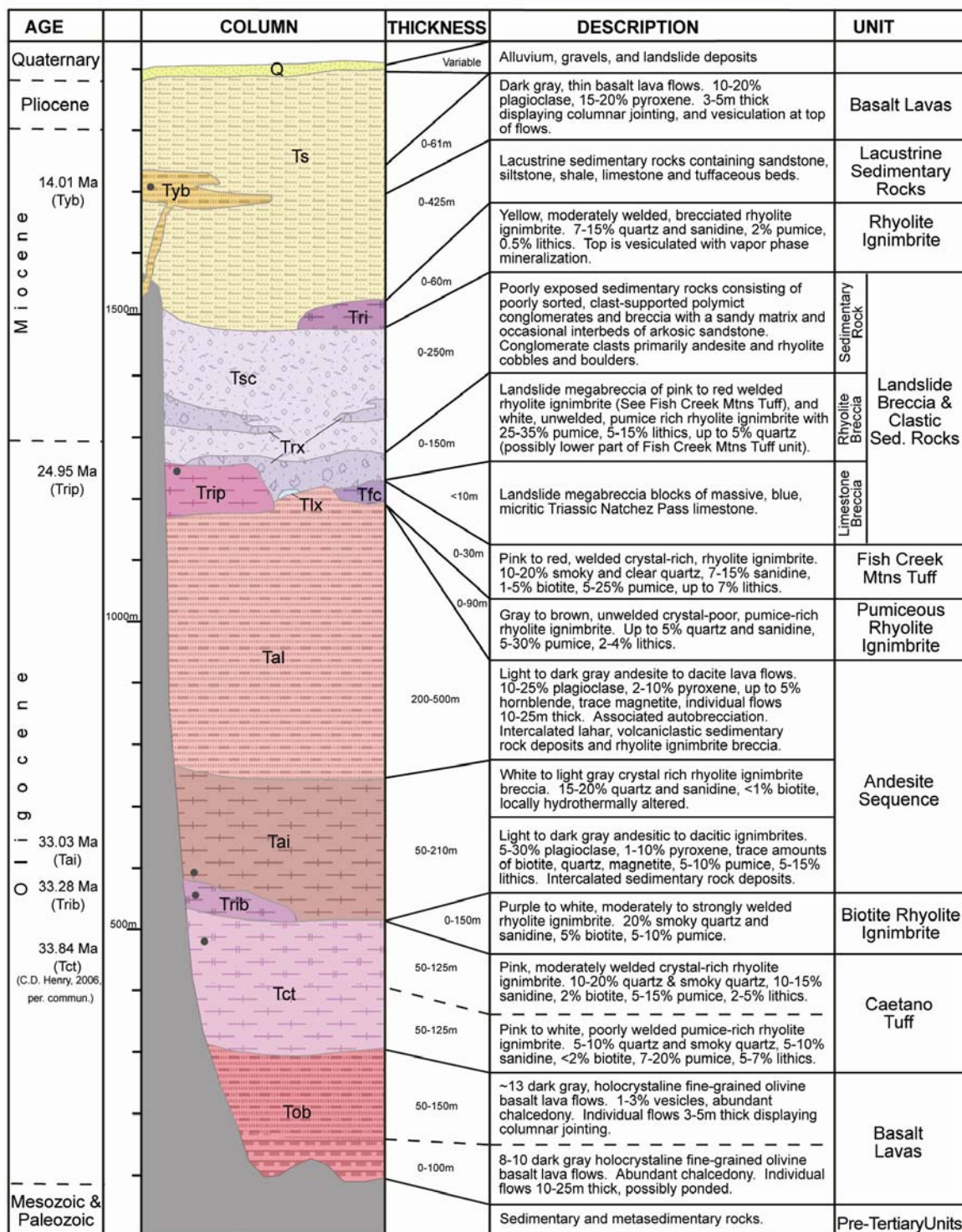


Figure 7. Generalized stratigraphic section of Cenozoic rocks in the Golconda Canyon area of the Tobin Range, Nevada. Stratigraphic location of samples used for $^{40}\text{Ar}/^{39}\text{Ar}$ dating identified with dot.

Caetano Tuff

The Caetano Tuff overlies the basalt and consists of moderately crystal-rich, poorly to moderately welded rhyolite ignimbrite. The Caetano Tuff is late Eocene to early Oligocene in age, based on numerous age determinations that range between 32 and 34.5 Ma (Naeser and McKee, 1970; John et al., 2003). John and Henry (2005) propose that there are two distinct ages and therefore two eruptive units for the Caetano Tuff. With $^{40}\text{Ar}/^{39}\text{Ar}$ dating on sanidine, they determined an age of 33.84 - 33.77 Ma for intracaldera exposures in the Shoshone Range, approximately 50 km east of the Tobin Range. Caetano Tuff samples lying north of the caldera have yielded ages between 34.5 and 34.2 Ma. C.D. Henry (personal commun, 2006) has obtained an age of 33.82 ± 0.07 Ma for sanidine from the Caetano Tuff in Golconda Canyon, confirming that the Tobin Range and Shoshone Range caldera samples of the Caetano Tuff have the same age. The geochemical composition of samples in Golconda Canyon is most similar to the composition of intracaldera samples in the Shoshone Range as well (John and Henry, 2005; this study). On the basis of age and chemical composition the Caetano Tuff of the Tobin Range is correlated with the intracaldera exposures of the Shoshone Range.

The source area for the older Caetano Tuff is unknown, however, John and Henry (2005) have identified the Shoshone Range exposures of the Caetano Tuff as a caldera that is the source area for the younger Caetano Tuff. Here the Caetano Tuff is very thick and displays multiple cooling units (Naeser and McKee, 1970; John and Henry, 2005). Based on age and geochemistry similarities, exposures in Golconda Canyon are the only identified outflow from the caldera (John and Henry, 2005).

Biotite Rhyolite Ignimbrite

Above the Caetano Tuff lies a moderately welded, crystal-rich, rhyolite ignimbrite with abundant biotite and moderately abundant pumice. This biotite rhyolite ignimbrite is seen as rare, isolated exposures in the field area where its stratigraphic position was uncertain: in some exposures it appears to underlie the andesite, and in other exposures to overlie. An $^{40}\text{Ar}/^{39}\text{Ar}$ age on sanidine of 33.28 ± 0.22 Ma (Table 1), indicates that this unit is older than the basal ignimbrites of the andesite sequence and therefore its strata position is placed between the Caetano Tuff and the andesite sequence.

Andesite

A thick sequence of up to 700 m of andesitic rocks overlies the Caetano Tuff in most exposures. The general stratigraphy consists of a basal series of biotite-pyroxene phyric ignimbrites; a thick series of pyroxene-phyric andesitic lava flows with intercalated lahars; and locally at the top of the section, a series of volcanoclastic sandstones and conglomerates. A number of lava flows at the top of the sequence are prominent ridge formers and are distinct due to large hornblende phenocrysts or abundant vesicles. Minor amounts of rhyolite ignimbrite landslide breccia are seen in both the andesite ignimbrites and in the lower portion of the pyroxene-phyric lava flows.

Few ages have been determined for the andesite sequence. McKee et al., (1971) report a K-Ar age, near the bottom of the andesite stratigraphy, of approximately 32 Ma. Likewise, sample TR-9 yielded an $^{40}\text{Ar}/^{39}\text{Ar}$ plateau age of

33.03 \pm 0.25 Ma on plagioclase from a vitrophyric ignimbrite near the base of the sequence (Table 1). Plagioclase from an andesite lava near the top of the sequence, sample TR-81, was dated but did not develop an age plateau. This sample generated a U-shaped pattern of argon release indicating excess argon in the sample.

Numerous dacitic and andesitic dikes are associated with the andesite sequence. Many of these intrusions likely intruded coeval with the formation of the andesite unit during the Oligocene, however, some dikes clearly postdate the end of andesite deposition. A northwest-striking dacitic dike in the southern part of the study area was emplaced along a fault that juxtaposes Oligocene andesite lavas adjacent to the base of the overlying Miocene sedimentary rocks, and these relations indicate that this intrusion post-dates andesitic volcanism here.

Late Oligocene Rhyolite Ignimbrites

Overlying the andesite sequence is a pumice-rich rhyolite ignimbrite. This gray to brown unwelded rhyolite is very crystal-poor, moderately lithic-rich and contains up to 30% pumice. An $^{40}\text{Ar}/^{39}\text{Ar}$ age determination on sanidine from a sample near the top of the unit has yielded a plateau age of 24.95 \pm 0.17 Ma (Table 1). This date constrains the upper age limit of the andesites.

This pumice-rich rhyolite unit may be correlative to the 4th cooling unit of the Bates Mountain Tuff of central and eastern Nevada, which is likewise correlative to the Nine Hills Tuff in western Nevada and eastern California. Sargent and McKee (1969) have described the Bates Mountain Tuff as being a crystal-poor ash flow tuff with phenocrysts of sanidine, quartz and lesser amounts of plagioclase, with varying

degrees of welding. $^{40}\text{Ar}/^{39}\text{Ar}$ age determinations by Deino (1989) on samples from both the Nine Hill Tuff and the Bates Mountain Tuff have produced a mean age of 25.11 ± 0.017 Ma (with mean ages of the samples varying by only 40,000 years). Whole rock geochemistry compiled by Deino (1985) is compared with geochemistry from the pumice-rich rhyolite in the Rhyolite Geochemistry section.

Also overlying the andesite sequence is the Fish Creek Mountains Tuff (FCMT), a quartz- and sanidine-rich, lithic-poor, moderately to strongly welded rhyolite ignimbrite up to ~15 m thick. A few ridge-forming exposures of FCMT can be traced a few hundred meters with consistent attitudes of compaction foliation, whereas many other exposures are brecciated, crop out as slope-formers, and contain diverse attitudes of compaction foliation. Whether the latter are in place or not is debatable, and is further discussed in the sedimentary rock and rhyolite landslide breccia unit description. The type locality and source area of this ash-flow tuff is a caldera complex in the Fish Creek Mountains (Burke and McKee, 1979), 10 km east of the southern Tobin Range. The FCMT in the type location has an age of 24.6 ± 1.3 Ma determined from fission-track dating on zircon (McKee et al., 1971). An age of 24.64 ± 0.07 Ma from $^{40}\text{Ar}/^{39}\text{Ar}$ dating on sanidine has also been determined for the FCMT (C.D. Henry, personal comm., 2006).

In the type locality of the Fish Creek Mountains Range (Figure 1) the FCMT has two cooling units. The lower unit is poorly to moderately welded, poorly to moderately crystal-rich, lithic-rich and grades upward into the upper cooling unit, which is strongly welded, crystal-rich and lithic-poor. Based on lithology, exposures in the southern Tobin Range correlate with the upper cooling unit of the type locality.

Syntectonic Sedimentary Rocks and Breccia

A map unit of sedimentary rock and landslide breccia (Tsc/Trx) overlies the FCMT and the pumice-rich rhyolite ignimbrite. Two distinct rhyolitic lithologies are evident and dominate the clasts present in the landslide breccia in the southern Tobin Range. One lithology is a red, crystal-rich, strongly welded, lithic- and pumice-poor rhyolite ignimbrite, similar to in situ exposures of FCMT in the Tobin Range. The other rock-type is a hydrothermally altered, whitish, poorly welded lithic- and pumice-rich, crystal-poor, vesicular rhyolite ignimbrite which may be correlative to the lithic and pumice-rich lower cooling unit of the FCMT. No exposures of this rhyolitic ignimbrite have been found as in situ in the Tobin Range. Also present as landslide breccia are localized blocks of limestone derived from the Natchez Pass formation.

The sandstones and conglomerates associated with the landslide breccia are usually poorly exposed in areas of subdued topography with abundant andesite and rhyolite cobbles and boulders lying within clay-rich soil. The sandstones are typically poorly sorted whereas the conglomerates are dominated with clasts of rhyolite and andesite, with lesser amounts of material derived from neighboring pre-Tertiary rocks. These sedimentary rocks are generally localized in the hangingwall of a major northwest-trending normal fault and appear considerably thicker in the northwest corner of the study area.

This map unit has been previously mapped on both the geologic maps of Pershing County (Tatlock et al., 1977) and the southern Tobin Range (Burke, 1973) as in situ exposures of FCMT and as sandstones and conglomerates associated with the andesite sequence. Field exposures examined in this study support an interpretation

that most FCMT exposures in the Tobin Range are landslide breccia deposits and have been displaced from their original depositional position. These exposures consist primarily of unconsolidated clay-rich volcanoclastic materials containing angular cobbles, boulders, or large blocks up to 7 m in diameter. From one block to the next, orientations of fiamme vary in a random pattern and indicate rotation of blocks relative to original depositional position. Many of these deposits lie in the hanging wall (south side) of a northwest striking normal fault that extends across the range. These observations suggests that most FCMT deposits in the Tobin Range are not the result of primary deposition, but rather, are secondary transported deposits associated with normal faulting. On the geologic map (Plate 1; Figure 3), areas dominated by rhyolite landslide breccia (Trx) are distinguished from those areas dominated by clastic sedimentary rock (Tsc) by a very approximately located contact.

Younger Rhyolite

Overlying the sedimentary rock and landslide breccia unit is an isolated exposure of moderately welded, crystal-rich, lithic poor rhyolite ignimbrite with vapor phase mineralization near the top of the unit.

Lacustrine Sedimentary Rocks and Younger Basalt

Stratigraphically above this rhyolite ignimbrite is a thick sequence of lacustrine sediments. This unit consists of tuffaceous siltstone, mudstone, and sandstone with minor limestone. Deffeyes (1959) provides a detailed study of these rocks in Jersey Valley and estimated a thickness of over 820m for this unit. Based on fossils within

the unit, an age of 15 Ma to 4 Ma has been determined (Deffeyes, 1959). Interbedded near the middle of the unit are a series of basalt lava flows. A whole-rock $^{40}\text{Ar}/^{39}\text{Ar}$ plateau age of 14.01 ± 0.12 Ma was determined for a basalt. Additional basalt exposures are seen in the study area southwest of Needle Peak and consist of lava flows and associated dikes that intrude late Oligocene normal faults.

Quaternary Deposits

Quaternary units consist of alluvium, landslide deposits and gravel deposits. Some gravel deposits consist of clasts primarily derived from the Pumpnickel and Havallah Formations and are localized near the base of the major northwest-southeast striking normal fault.

Rhyolite Geochemistry

Whole rock geochemical analyses were obtained on ten rhyolite samples. Plots of the abundances of immobile elements in the samples were for comparison with one another and to values from published literature of tuffs in central Nevada (Figure 8). The Caetano Tuff and biotite rhyolite ignimbrite both have lower amounts of immobile elements present, and based on available radiometric ages, were deposited in a short period of time (~33.8 – 33.3 Ma). Because the biotite rhyolite ignimbrite contains abundant biotite, it is possible that this unit is a younger eruption from the Caetano Tuff magma chamber that has not been recognized elsewhere. The biotite rhyolite ignimbrite is enriched in incompatible elements compared to the Caetano Tuff, possibly as a result of magma depletion from previous eruptions.

However, samples from the Caetano Tuff show increasing Zr up-section, whereas the biotite rhyolite ignimbrite does not continue this trend of increasing Zr values.

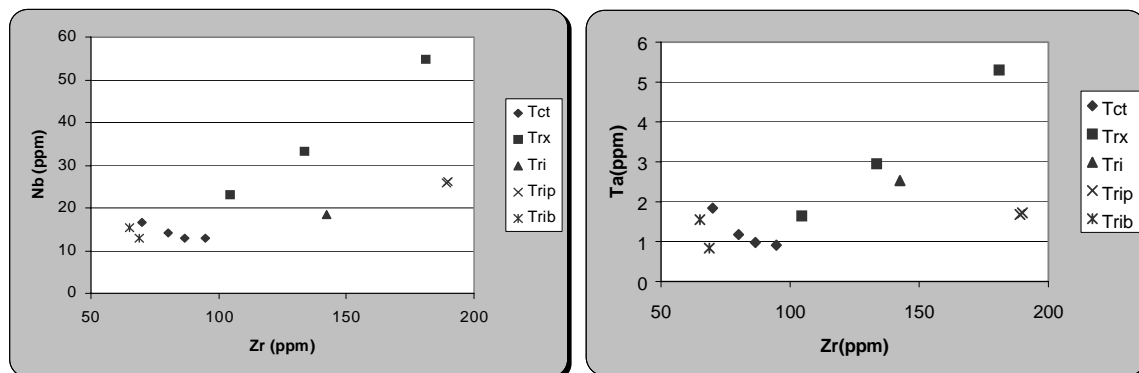


Figure 8. Whole rock geochemistry plots for rhyolite ignimbrite samples. Tct – Caetano tuff (33.8 Ma), Trx – rhyolite landslide breccia (<24.6, >14 Ma), Tri – rhyolite ignimbrite, Trip – pumice-rich rhyolite ignimbrite (24.9 Ma), Trib – biotite-rich rhyolite ignimbrite (33.3 Ma).

Samples from the rhyolite landslide breccia, which were originally derived from the Fish Creek Mountains Tuff, show increasing amounts of Hf, Nb, Y, Ta, and Th with increasing Zr. No published data are available with whole rock geochemistry of immobile elements for the Fish Creek Mountains Tuff, though McKee (1970) has inferred whole rock values for Sr and Rb from known values of Sr, Rb and K in sanidine phenocrysts. McKee's (1970) values for Sr (65 ppm) and Rb (265 ppm) are similar to samples from the rhyolite landslide breccias analyzed here (Sr = 47-93 ppm, Rb = 199-440 ppm).

Based on unit descriptions and age determinations, the pumice-rich rhyolite could be correlative to the Bates Mountain and Nine Hill Tuffs (see description in Cenozoic Rocks section). In Table 2, a list of values for a suite of immobile elements is compiled for the pumice-rich rhyolite and for the Nine Hill and Bates Mountain

Tuffs (Deino, 1985). The Nine Hill and Bates Mountain Tuffs are consistently similar in composition, whereas the pumice-rich rhyolite shares some similarities but also has some differences. Differences arise in Ba, Ce, La, Sr, and Zr. Most notable are the Zr values which are twice as high in the Nine Hill and Bates Mountain Tuffs (~400 ppm), compared to the pumice-rich rhyolite (~200 ppm). Enrichment of Zr in the Nine Hill and Bates Mountain Tuffs is a distinctive characteristic of these units, and the pumice-rich rhyolite generally has half as much Zr. Based on the geochemical mismatch and $^{40}\text{Ar}/^{39}\text{Ar}$ ages, the pumice-rich rhyolite ignimbrite is not equivalent to the Nine Hill and Bates Mountain Tuffs and represents a slightly younger alkali rhyolite tuff.

Table 2. Whole rock geochemistry values.

	TR05-27	TR05-21	Nine Hill	Bates Mtn
Ba	700	590	179 \pm 16	167 \pm 49
Ce	81	88	121 \pm 4	130 \pm 5
Ga	21	18.35	21.8 \pm 0.3	22 \pm 1
La	38	44.5	66 \pm 2	64 \pm 3
Nb	26	26.1	29.9 \pm 0.3	30.5 \pm 0.3
Pb	32	137.5	22 \pm 2	47 \pm 2
Sr	109.5	77.7	26 \pm 2	33 \pm 16
Th	19	21.4	28.8 \pm 0.5	27 \pm 1
Y	24.3	30.3	41.2 \pm 0.9	40 \pm 1
Zn	72	47	64 \pm 4	101 \pm 2
Zr	189	190	399 \pm 3	406 \pm 4

TR05-27 and TR05-21 from the pumice-rich rhyolite unit (Trip) and average values for the Nine Hill and Bates Mountain Tuffs. All values in ppm. Values for Nine Hill and Bates Mountain Tuffs from Deino (1985).

NORMAL FAULTS AND TIMING OF EXTENSION

Normal faults in the Golconda Canyon region of the Tobin Range principally strike north-south and dip steeply to moderately to the west. Predominantly westward dipping faults have produced eastward tilting, thus resulting in eastward dipping Tertiary rocks. Three main groups of faults were identified and are described below. Figure 9 schematically illustrates the sequence of faulting.

Early Oligocene Faults

Throughout the Tertiary paleo-valley, numerous, small faults with dips ranging from $\sim 35^\circ$ to 80° to the west have been identified (Figure 10). These faults generally strike north or northeast, though occasionally east-west, and are truncated by a major northwest-striking fault.

The timing of this set of faults is best determined by relationships seen in the andesite sequence in the western part of the study area. The andesitic rocks dip from $\sim 15^\circ$ to 45° to the east. Steeper dipping ignimbrites ($\sim 25^\circ$ - 35°) underlie lava flows with shallower dips ($\sim 15^\circ$ - 20°). One particular fault offsets the basal ignimbrites but not the upper lava flows and hence is buried by the latter. These relationships indicate a period of faulting synchronous with and extending a short time after the ignimbrite volcanism, dated here at 33.03 Ma, but prior to lava flow deposition. Thus, this early faulting resulted in $\sim 5^\circ$ to 20° of eastward tilting of the andesite ignimbrites. Additionally, minor amounts of rhyolite breccias are seen in the andesite sequence and were likely deposited syntectonically with this phase of faulting.

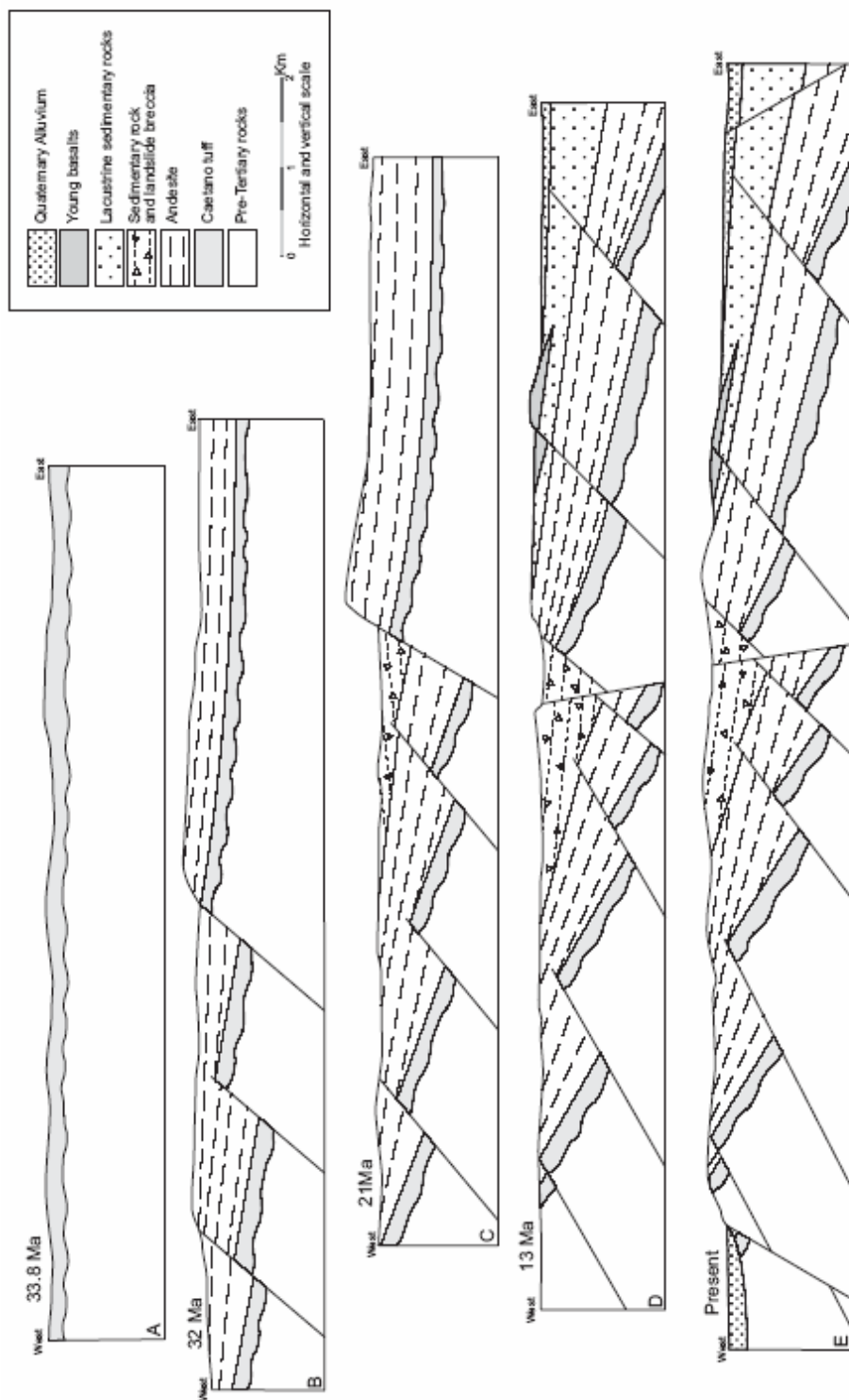


Figure 9. Schematic cross-sections showing a time-sequence of extensional faulting in the Tobin Range. A) Deposition of Caetano Tuff (33.8 Ma) prior to extensional faulting, B) Late Oligocene extension in western part of range coeval with deposition of andesite ignimbrites (33 Ma) and lavas, C) development of major northwest striking fault and deposition of syntectonic sedimentary rock and landslide breccias (between 24.6 and 14 Ma), D) extensional faulting in eastern part of range resulting in eastward dipping units, including 14 Ma basalts, and development of steeply eastward dipping faults. E) Late Cenozoic faulting along the margins of the Tobin Range.

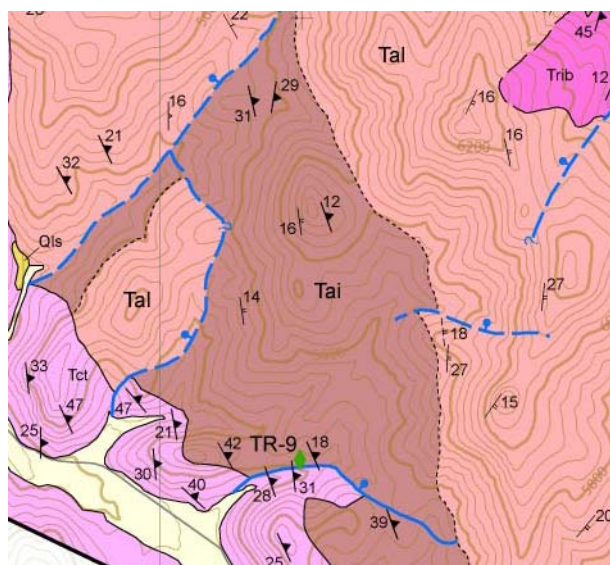


Figure 10. Geologic map showing examples of early Oligocene faults. Note the southern most fault which cuts the andesite ignimbrite (Tai) but does not cut the andesite lavas (Tal)

Late Oligocene to Middle Miocene Faults

A major northwest-striking normal fault crosses the Tobin Range and both offsets and locally forms the northern boundary of the Tertiary paleo-valley. This fault strikes approximately N30°W, though becomes more east-west striking on the eastern side of the range, and has dips ranging from ~50° to 55° to the southwest. Palinspastic restorations suggest that this fault has accommodated locally more than 1.7 km of normal displacement. Movement on this fault has resulted in the juxtaposition of pre-Tertiary rocks against Tertiary volcanic units and has localized much of the Tertiary sedimentary rock and landslide breccia unit in the hangingwall. Deposits of Quaternary gravels, consisting largely of pre-Tertiary sediments, have also been localized in the hangingwall. Field relationships suggest that the gravels are not syntectonic, but rather, were localized in the hangingwall as a result of later erosion.

The age of this fault system is constrained by the onset of sedimentary rock and landslide breccia deposition which began sometime after the deposition of the FCMT (24.64 Ma) and prior to the eruption of the younger Tertiary basalts (14.01 Ma), which overlie the fault.

Middle Miocene and Younger Faults

Faults middle Miocene or younger in age strike north-south, dip moderately to the west, and offset the 14.01 Ma basalts that dip $\sim 25^\circ$ to 30° E in the eastern part of the study area. The dips of the basalts are a result of movement on these faults and active faults along the east side of Jersey Valley. The dips of these basalts are similar to the magnitude of dips of early Oligocene volcanic rocks to the west, near the mouth of Golconda Canyon, that were affected by the older Oligocene phase of faulting. This comparison suggests that this younger phase of normal faulting did not affect the western area.

Also present in the eastern part of the Tobin Range are eastward dipping faults that appear to be middle Miocene in age. One particular fault forms a contact between the Caetano Tuff and the andesite sequence, has a northeasterly strike and dips steeply to the east (Figure 11). This fault postdates and offsets the major late Oligocene northwest striking fault. Because it has a similar orientation, this fault may be related to the fault bounding the eastern limit of the Tobin Range. This fault is significant because displacement along east-dipping faults would cause westward tilt and diminish the magnitude of the eastward dip of the Tertiary rocks.

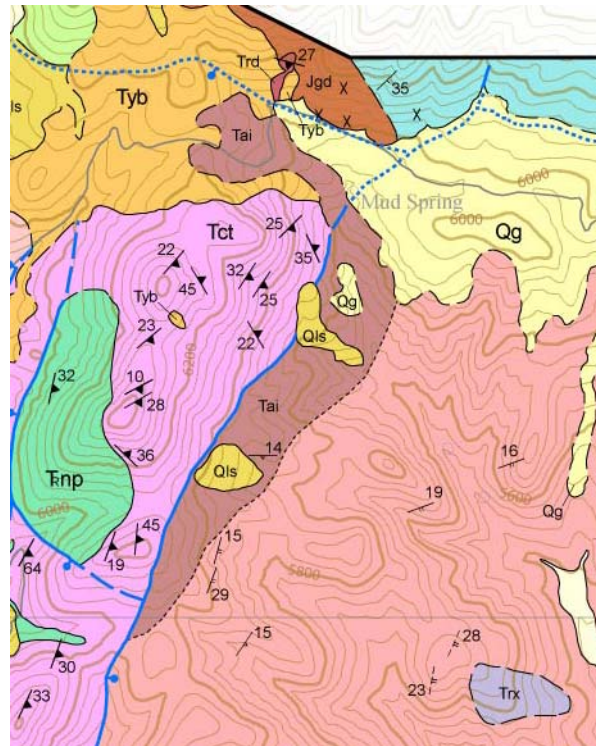


Figure 11. Geologic map showing example of a steeply east dipping middle Miocene or younger fault. This fault marks the contact between the Caetano Tuff (Tct) and the andesite sequence (Tai and Tal). Note inferred offset of the late Oligocene fault (north end of map, striking west-northwest) as result of movement on the east dipping fault.

A subset of the younger faults described above are faults that have evidence of Pleistocene or Holocene movement. The youngest faults are those bounding either side of the Tobin Range. The western limit of the Tobin Range is bounded by a large west-dipping normal fault that ruptured during the 1915 Pleasant Valley earthquake. The Pleasant Valley earthquake is the most northerly surface-rupturing event in the Central Nevada Seismic Zone to have occurred during historical times. A detailed study by Wallace (1984) documents the surface rupture of this event. Average vertical displacement along the scarps was 2 m with a maximum displacement of 5.8 m occurring along the most southerly scarp, near the mouth of Golconda Canyon

(Wallace, 1984). Lateral displacement was minimal, but when present was right-lateral. Wallace (1984) reported a maximum lateral displacement of two meters just north of Golconda Canyon. Recurrence intervals for the Pleasant Valley fault are estimated between approximately 5,000 to less than 12,000 years (Wallace, 1984; Bonilla et al., 1984).

The eastern limit of the Tobin Range in the northeast corner of the map area, and continuing north along the margin of Buffalo Valley, is bounded by a large normal fault dipping to the east. The displacement on this fault dies out as it extends south into Jersey Valley, and displacement appears to be transferred across the valley to the normal fault bounding the western margin of the Fish Creek Mountains.

DISCUSSION

Timing and Amount of Extension

Extension of the Basin and Range Province has occurred by means of normal faulting, and has resulted in the characteristic topography of horsts and grabens (Stewart, 1978; Spencer and Reynolds, 1986; Dickinson, 1991). Single generations of normal faulting, with steep dips of approximately 50° to 60° , can account for 10-20% total extension of terranes (Stewart, 1978; Lerch et al., 2004; Colgan et al., 2006). Areas that have experienced greater amounts of extension, in many places exceeding 100%, have undergone more complex normal faulting in which at least two successive generations of normal faults have taken place (Proffett, 1977). Where all faults dip the same direction, successive crosscutting by younger faults has caused inactive older normal faults to rotate to shallower dips. The result is highly extended terranes with shallowly dipping normal faults and steeply dipping units. Areas of high extension have also been described together with the presence of low-angle detachment faults (Davis and Lister, 1988). However, detachment faults have not been identified in many areas that have experienced large amounts of extension in volcanic terranes of western Nevada, such as the Yerington district and the El Dorado mountains (Anderson, 1971; Proffett, 1977).

For a single generation of normal faults, the amount of extension can be calculated from the average dip of the rock units and an estimate of the initial dip of the normal faults by using the following equation from Thompson (1960)

$$e=100\left(\frac{\sin\theta}{\sin(\theta-\phi)}-1\right)$$

where e is the amount of extension in percent, θ is the original dip of normal faults and ϕ is the dip of rock units that were flat prior to faulting.

The Tertiary rock units in the Golconda Canyon area have dips that range between 15° and 40° to the east. The average dip in the area is ~25°, and this amount of dip is relatively consistent throughout the range. If we assume that all of the normal faults initiated with a dip of 60° and use an average dip of 25° for the rock units, east-west crustal extension in the Tobin Range is calculated to be 51%. This calculation provides a rough estimate but does not adequately accommodate multiple generations of faults or faults which dip in the same direction as the rock units which may decrease the average dip of the rocks used in the calculation.

A more accurate estimation of the amount of extension in the Tobin Range can be obtained from palinspastic restorations of cross-sections drawn parallel to the slip direction along the faults. Cross-section restorations have provided extension estimates between 40-45%. Because of factors such as erosion and faults for which the amount of displacement cannot be determined, these estimates provide a minimum percentage of extension and are consistent with the previously calculated percentage.

Regional Extension Comparisons

Estimates of extension in the Tobin Range agree with a pattern of decreasing amounts of extension to the northwest (Figure 12). Regional palinspastic restorations by Smith et al. (1991) suggest total amounts of crustal extension between 50-100% in central Nevada, and Hudson et al. (2000) estimate >100% extension for the Job Canyon caldera complex in the nearby southern Stillwater Range. To the northwest, workers have found extension on the order of 10-20% in the Black Rock and Pine Forest Ranges (Lerch et al., 2004; Colgan et al., 2006). Likewise, central Nevada and northwest Nevada see a difference in timing in normal fault inception (Figure 12). The Tobin Range, with normal fault initiation during the early Oligocene, and its multiple generations of faulting is consistent with work by Smith (1992) and Hudson et al. (2000) who identified at least two generations of normal faulting, beginning in the Oligocene in the Toiyabe and Stillwater Ranges. To the northwest, Colgan et al. (2006) have identified a single generation of normal faulting which began sometime after the late Miocene.

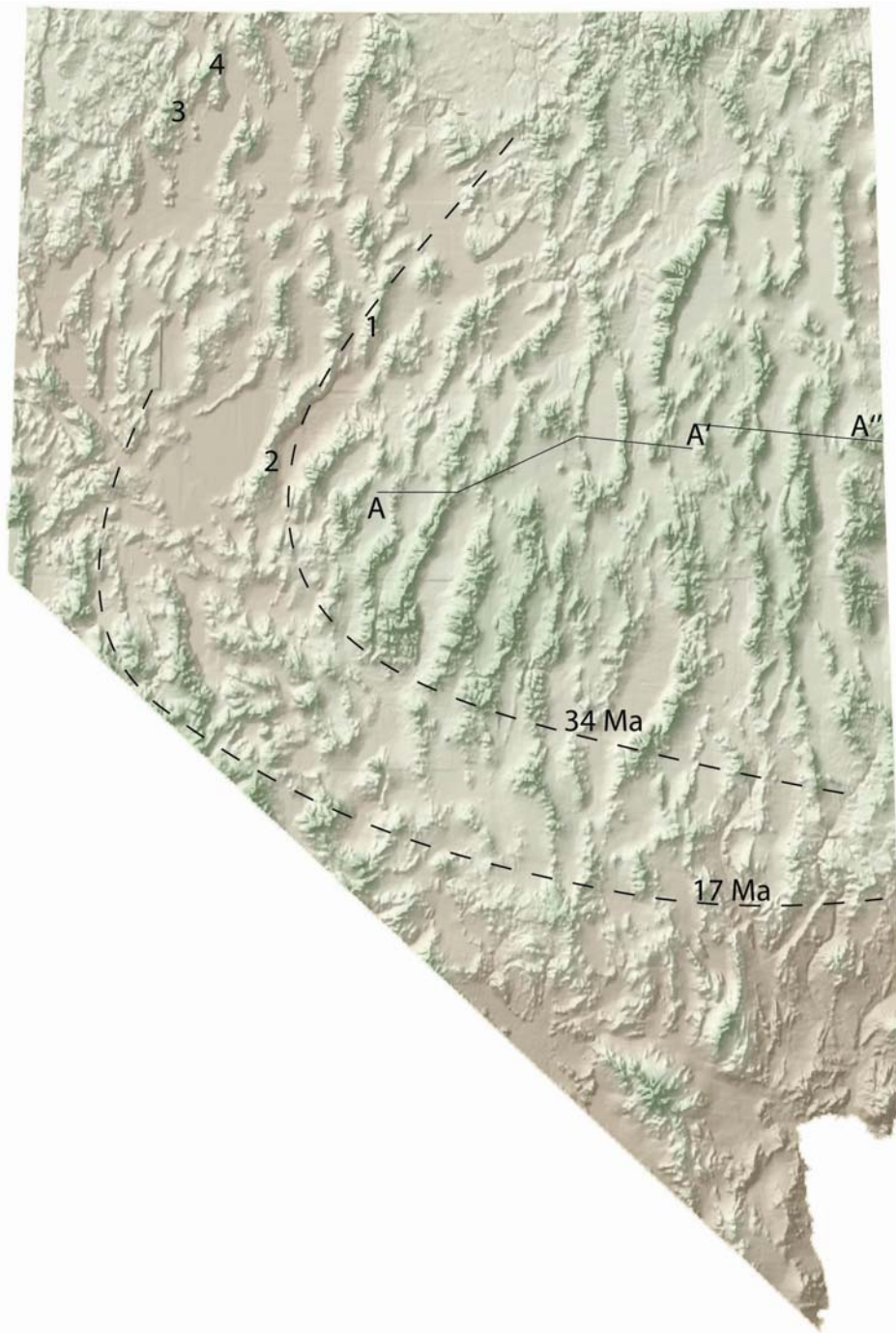


Figure 12. Shaded relief map of Nevada showing the location of estimates of extension. 1 – Tobin Range (50%; this study), 2 – southern Stillwater Range (>100%; Hudson et al., 2000), 3 – Black Rock Range (10%; Lerch et al., 2004) 4 – Pine Forest Range (15-20%; Colgan et al., 2006), A-A'' – regional cross sections across central Nevada (ave. 50%; Smith et al., 1991). Dashed lines indicate migration of areas of significant extension through time (modified from Seedorff, 1991).

CONCLUSION

Cenozoic extensional normal faulting has occurred since the early Oligocene in the Golconda Canyon area. The first phase of normal faulting developed coeval with the deposition of the andesite sequence (~33 Ma), and is consistent with the regional pattern of westward younging normal fault inception in northwest Nevada. During this phase, faults were principally localized in the western part of the range. The second phase of faulting resulted in the development of a steeply dipping northwest-striking fault that was active from the late Oligocene until the middle Miocene. This fault is responsible for the localization of syntectonic clastic sedimentary rocks and rhyolitic breccias, which accumulated in the hangingwall of the fault. Postdating the northwest-trending fault is a series of faults that are younger than middle Miocene age and are confined to the eastern part of the range. These faults are primarily west dipping though some faults dip to the east. This period of faulting resulted in a similar amount of tilting, and likely extension, as had occurred to the west during the time of andesite deposition. The last set of faults include normal faults that are active today in the form of steeply dipping range front faults that bound either side of the Tobin Range.

Total crustal extension for the Tobin Range is estimated to be approximately 50%. This estimate of extension is consistent with other estimates for central Nevada and areas further to the east, as opposed to areas to the northwest, where extension diminishes to 10-20%.

REFERENCES

- Anderson, R.E., 1971, Thin skin distension in Tertiary rocks of southeastern Nevada: *Geologic Society of American Bulletin*, v. 82, p. 43-58.
- Best, M.G., and Christiansen, E.H., 1991, Limited extension during peak Tertiary volcanism, Great Basin of Nevada and Utah: *Journal of Geophysical Research*, v. 96, n. B8, p. 13,509-13,528.
- Blackwell, D.D., Steele, J.L., and Carter, L.S., 1991, Heat-flow patterns of the North American continent; a discussion of the geothermal map of North America, in Slemmons, D.B., Engdahl, E.R., Zoback, M.D., Blackwell, D.D., eds. *Neotectonics of North America, the Decade of North American Geology Project series: Geologic Society of America*, p. 423-436.
- Block, L., and Royden, L.H., 1990, Core complex geometries and regional scale flow in the lower crust: *Tectonics*, v. 9, no. 4, p. 557-567.
- Bonilla, M.G., Villalobos, H.A., and Wallace, R.E., 1984, Exploratory trench across the Pleasant Valley Fault, Nevada: *U.S. Geological Survey Professional Paper 1274-B*, p. B1-B14.
- Burke, D.B., 1973, Reinterpretation of the Tobin thrust – Pre-Tertiary geology of the southern Tobin Range, Pershing County, Nevada: Ph.D. thesis, Stanford University, Stanford, Calif.
- Burke, D.B., and McKee, E.H., 1979, Mid-Cenozoic volcano-tectonic troughs in central Nevada: *Geologic Society of America Bulletin, Part I*, v. 90, p.181-184.
- Catchings, R.D., and Mooney, W.D., 1991, Basin and Range crustal and upper mantle structure, northwest to central Nevada: *Journal of Geophysical Research*, v. 96, n. B4, p. 6247-6267.
- Christiansen, R.L., and McKee, E.H., 1978, Late Cenozoic volcanic and tectonic evolution of the Great Basin and Columbia Intermontane regions, in Smith, R.B., and Eaton, G.P., eds. *Cenozoic tectonics and regional geophysics of the western Cordillera: Memoir – Geologic Society of America*, i. 152, p. 283-311.
- Colgan, J.P., Dumitru, T.A., McWilliams, M., and Miller, E.L., 2006, Timing of Cenozoic volcanism and Basin and Range extension in northwestern Nevada: New constraints from the northern Pine Forest Range: *Geologic Society of American Bulletin*, v. 118, n.1/2, p. 126-139.

- Dalrymple, G.B., and Lanphere, M.A., 1974, $^{40}\text{Ar}/^{39}\text{Ar}$ age spectra of some undisturbed terrestrial samples: *Geochimica et Cosmochimica Acta*, v. 38, p. 715-738.
- Davis, G.A., and Lister, G.S., 1988, Detachment faulting in continental extension: Perspectives from the southwestern U.S. Cordillera, in Clark, S.P., Jr., ed., *Processes in continental lithospheric deformation: Geologic Society of America Special Paper 218*, p.133-159.
- Deffeyes, K.S., 1959, Late Cenozoic sedimentation and tectonic development of central Nevada: Ph.D. thesis, Princeton University, Princeton, N.J.
- Deino, A.L., 1985, I. Stratigraphy, chemistry, K-Ar dating, paleomagnetism of the Nine Hill tuff, California-Nevada, II. Miocene/Oligocene ash-flow tuffs of Seven Lakes Mountain, California-Nevada, III. Improved calibration methods and error estimates for K-Ar dating: Ph.D. thesis, University of California, Berkeley.
- Deino, A.L., 1989, Single-crystal $^{40}\text{Ar}/^{39}\text{Ar}$ dating as an aide in correlation of ash flows: examples from the Chimney Spring/New Pass tuffs and the Nine Hill/Bates Mountain tuffs of California and Nevada: *Bulletin – New Mexico Bureau of Mines and Mineral Resources*, p. 70.
- DePolo, C.M., Clark, D.G., Slemmons, D.B., and Ramelli, A.R., 1991, Historical surface faulting in the Basin and Range province, western North America: implications for fault segmentation: *Journal of Structural Geology*, v. 13, n. 2, p. 123-136.
- Dickinson, W.R., 1991, Tectonic setting of faulted Tertiary strata associate with the Catalina core complex in southern Arizona: *Geologic Society of America Special Paper 264*, 106, p.
- Duncan, R.A., Hooper, P.R., Rehacek, J., Marsh, J.S., and Duncan, A.R., 1997, The timing and duration of the Karoo igneous event, southern Gondwana: *Journal of Geophysical Research*, v. 102, no. B8, p. 18,127-18,138.
- Duncan, R.A., and Keller, R.A., 2004, Radiometric ages for basement rocks from the Emperor Seamounts, ODP Leg 197: *Geochemistry, Geophysics, Geosystems*, v. 5, n. 8, Q08L03, doi:10.1029/2004GC000704.
- Ferguson, H.G., Roberts, R.J., and Muller, S.W., 1952, *Geology of the Golconda quadrangle, Nevada*: U.S Geological Survey Geol. Quad. Map GQ-15.

- Frey, H.M., Lange, R.A., Hall, C.M., and Delgado-Granados, H., 2004, Magma eruption rates constrained by $^{40}\text{Ar}/^{39}\text{Ar}$ chronology and GIS for the Ceboruco-San Pedro volcanic field, western Mexico: *Geologic Society of America Bulletin*, v. 116, p. 259-276.
- Gans, P.B., 1987, An open-system, two-layer crustal stretching model for the eastern Great Basin: *Tectonics*, v. 6, n. 1, p. 1-12.
- Gans, P.B., Mahood, G.A., and Schermer, E., 1989, Synextensional magmatism in the Basin and Range Province; a case study from the eastern Great Basin: *Geologic Society of America Special Paper* 233, 53, p.
- Gianella, V.P., and Callagan, E., 1933, The Cedar Mountain, Nevada, earthquake of December 20, 1932: *Transactions – American Geophysical Union*, v. 13, i. 4, p. 257-260.
- Gianella, V.P., and Callagan, E., 1936, The earthquake of December 20, 1932, at Cedar Mountain, Nevada, and its bearing on the genesis of Basin Range structure: *Journal of Geology*, v. 42, i. 1, p. 1-22.
- Henry, C.D., Faulds, J.E., Garside, L.J., and Hinz, Nicholas, H., 2003, Tectonic implications of ash-flow tuffs and paleovalleys in the Western U.S: *Geologic Society of America, Abstracts with Programs*, v. 35, i. 6, p. 346.
- Hudson, M.R., John, D.A., Conrad, J.E., and McKee, E.H., 2000, Style and age of late Oligocene-early Miocene deformation in the southern Stillwater Range, west central Nevada: Paleomagnetism, geochronology, and field relations: *Journal of Geophysical Research*, v. 105, n.1, p. 929-954.
- John, D.A., Hofstra, A.H., Fleck, R.J., Brummer, J.E., and Saderholm, E.C., 2003, Geologic setting and genesis of the Mule Canyon low-sulfidation epithermal gold-silver deposit, north-central Nevada: *Economic Geology and the Bulletin of the Society of Economic Geologists*, v. 98, i. 2, p. 425-463.
- John, D.A., and Henry, C.D., 2005, Multiple units of the Caetano tuff, northern Nevada: caldera source and preliminary geochronology and geochemistry: *Geological Society of America, Abstracts with Programs*, V. 37, n. 7, p. 379.
- Klemperer, S.L., Hauge, T.A., Hauser, E.C., Oliver, J.E., and Potter, C.J., 1986, The Moho in the northern Basin and Range Province, Nevada, along the COCORP 40 N seismic reflection transect: *Geologic Society of America Bulletin*, v. 97, n. 5, p. 603-618.
- Koppers, A.A.P., 2002, ArArCALC – Software for Ar-40/Ar-39 age calculations, *Comput. Geosci.*, 28, p. 605-619.

- Lerch, D.W., McWilliams, M.O., Miller, E.L., and Colgan, J.P., 2004, Structure and magmatic evolution of the northern Black Rock Range, Nevada: Preparation for a wide-angle refraction/reflection survey: *Geologic Society of America, Abstracts with Programs*, v. 36, n. 4, p.37.
- Masursky, H., 1960, Welded tuffs in the northern Toiyabe Range, Nevada, in *Geological Survey research 1960: U.S. Geological Survey Professional Paper 400-B*, p. B281-B283.
- McKee, E.H., 1970, Fish Creek Mountains tuff and volcanic center, Lander County, Nevada: *U.S Geological Survey Professional Paper 681*.
- McKee, E.H., and Burke, D.B., 1972, Fission-track age bearing on the Permian-Triassic boundary and time of the Sonoma orogeny in north-central Nevada: *Geologic Society of America Bulletin*, v. 83, no. 7, p. 1949-1952.
- McKee, E.H., Silberman, M.L., Marvin, R.E., and Obradovich, J.D., 1971, A summary of radiometric ages of Tertiary volcanic rocks in Nevada and eastern California – Part 1, central Nevada: *Isochron/West*, n. 2, p. 21-42.
- McKenzie, D., Nimmo, F., Jackson, J.A., Gans, P.B., and Miller, E.L., 2000, Characteristics and consequences of flow in the lower crust: *Journal of Geophysical Research*, v.105, n. B5, p. 11,029-11,046.
- Muller, S.W., Ferguson, H.G., and Roberts, R.J., 1951, *Geology of the Mount Tobin quadrangle, Nevada: U.S. Geological Survey Geol. Quad. Map GQ-7*.
- Naeser, C.W., and McKee, E.H., 1970, Fission-track and K-Ar ages of Tertiary ash-flow tuffs, north-central Nevada: *Geologic Society of America Bulletin*, v. 81, p. 3375-3384.
- Proffett, J.M. Jr., 1977, Cenozoic geology of the Yerington district, Nevada, and implications for the nature and origin of Basin and Range faulting: *Geologic Society of America Bulletin*, v. 88, p. 247-266.
- Proffett, J.M. Jr., and Proffett, B.H., 1976, Stratigraphy of the Tertiary ash flow tuffs in the Yerington district, Nevada: *Nevada Bureau of Mines and Geology – Report*, i. 27.
- Renne, P.R., Deino, A.L., Walter, R.C., Turrin, B.D., Swisher, C.C., Becker, T.A., Curtis, G.H., Sharp, W.D., Jaouni, A., 1994, Intercalibration of astronomical and radioisotopic time: *Geology*, v. 22, i. 9 p. 783-786.
- Sargent, K.A., and McKee, E.H., 1969, The Bates Mountain tuff in northern Nye County, Nevada: *U.S. Geological Survey Bulletin*, p. E1-E12.

- Seedorff, E., 1991, Magmatism, extension, and ore deposits of Eocene to Holocene age in the Great Basin; mutual effects and preliminary proposed genetic relationships: in Raines, G.L., Lisle, R.F., Schafer, R.W., and Wilkinson, W.H., eds., *Geology and ore deposits of the Great Basin: Geologic Society of Nevada*, April 1-5, Reno, NV, p. 133-178.
- Slemmons, D.B., 1957, Geologic effects of the Dixie Valley-Fairview Peak, Nevada, earthquakes of December 16, 1954: *Bulletin of the Seismological Survey of America*, v. 47, i. 4 p. 353-375.
- Smith, D.L., 1992, History and kinematics of Cenozoic extension in the northern Toiyabe Range, Lander County, Nevada: *Geologic Society of America Bulletin*, v. 104, p. 789-801.
- Smith, D.L., Gans, P.B., Miller, E.L., Lisle, R.E., Schafer, R.W., and Wilkinson, W.H., 1991, Palinspastic restoration of Cenozoic extension in the central and eastern Basin and Range Province at latitude 30-40 degrees N: in Raines, G.L., Lisle, R.F., Schafer, R.W., and Wilkinson, W.H., eds., *Geology and ore deposits of the Great Basin: Reno, Nevada, Geological Society of Nevada*, p. 75-86.
- Spencer, J.E., and Reynolds, S.J., 1986, Some aspects of the middle Tertiary tectonics of Arizona and southeastern California: *Arizona Geologic Society Digest*, v. 16, p. 102-107.
- Stewart, J.H., 1978, Basin-range structure in western North America: A review: *Geologic Society of America Memoir*, i. 152, p. 1-31.
- Tatlock, D.B., Johnson, M.G., Burke, D.B., and Stewart, J.H., 1977, Geologic Map of Pershing County, Nevada, 1:250,000, in Johnson, M.G., ed., *Geology and mineral deposits of Pershing County, Nevada: Nevada Bureau of Mines and Geology Bulletin*, n. 89.
- Tegnar, C., and Duncan, R.A., 1999, $^{40}\text{Ar}/^{39}\text{Ar}$ chronology for the volcanic history of the southeast Greenland rifted margin: in Larsen, H.C., Duncan, R.A., Allan, J.F., Brooks, K., eds., *Proceedings of the Ocean Drilling Program, Scientific Results*, v. 163, p. 53-62.
- Thompson, G.A., 1960, Problem of Late Cenozoic Structure of the Basin and Ranges: in Kvale, A., and Metzger, A., eds., *Structure of the earth's crust and deformation of rocks, Report of the twenty-first session Norden, International Geological Congress*, p. 62-68.
- Wallace, R.E., 1984, Fault scarps formed during the earthquakes of October 2, 1915, in Pleasant Valley, Nevada, and some tectonic implication: *U.S. Geological Survey Professional Paper 1274-A*, p. A1-A33.

- Wallace, R.E., 1984, Patterns and timing of late Quaternary faulting in the Great Basin province and relation to some regional tectonic features: *Journal of Geophysical Research*, v. 89, n. B7, p. 5763-5769.
- Wallace, R.E., 1987, Grouping and migration of surface faulting and variations in slip rates on faults in the Great Basin Province: *Bulletin of the Seismological Society of America*, v. 77, n. 3, p. 868-876.
- Wernicke, B.P., 1992, Cenozoic extensional tectonics of the U.S. Cordillera: in Burchfiel, B.C., Lipman, P.W., and Zoback, M.L., eds., *The Cordilleran Orogen: Conterminous U.S.: Decade of North American Geology*, Geologic Society of America, v. G-3, p. 553-581.
- Wernicke, B.P., 1990, The fluid crustal layer and its implications for continental dynamics, in Salisbury, M.H., Fountain, D.M., eds., *Exposed cross-sections of the continental crust*: Netherlands, Kluwer Publishers, p. 509-544.
- Wernicke, B.P., Axen, G.J., and Snow, J.K., 1988, Basin and Range extensional tectonics at the latitude of Las Vegas, Nevada: *Geologic Society of America Bulletin*, v. 100, p. 1738-1757.

APPENDIX

Radiometric Age Determinations

Plateau, K/Ca, isochron and inverse isochron plots created from the $^{40}\text{Ar}/^{39}\text{Ar}$ age analysis are in Figure 13. All radiometric data can be accessed on the enclosed CD. Sample preparation consisted of crushing, pulverizing, and sieving all samples to an appropriate mesh size for separating minerals. The sieved separates were then washed through a process of ultrasonic cleaning and decanting using de-ionized water. For samples TR-9 and TR-81, a Frantz isodynamic magnetic separator was used to extract magnetic crystals and groundmass until a concentration of plagioclase remained. The final concentrations of plagioclase were then handpicked to remove any remaining impurities in the samples. For samples TR05-21 and TR05-26, individual sanidine crystals were handpicked from the respective sieved separates. All samples were then washed using ultrasonic cleaning and decanting with 5% HNO_3 for 20 minutes, followed by 5% HF for 1 minute and de-ionized water for 15 minutes.

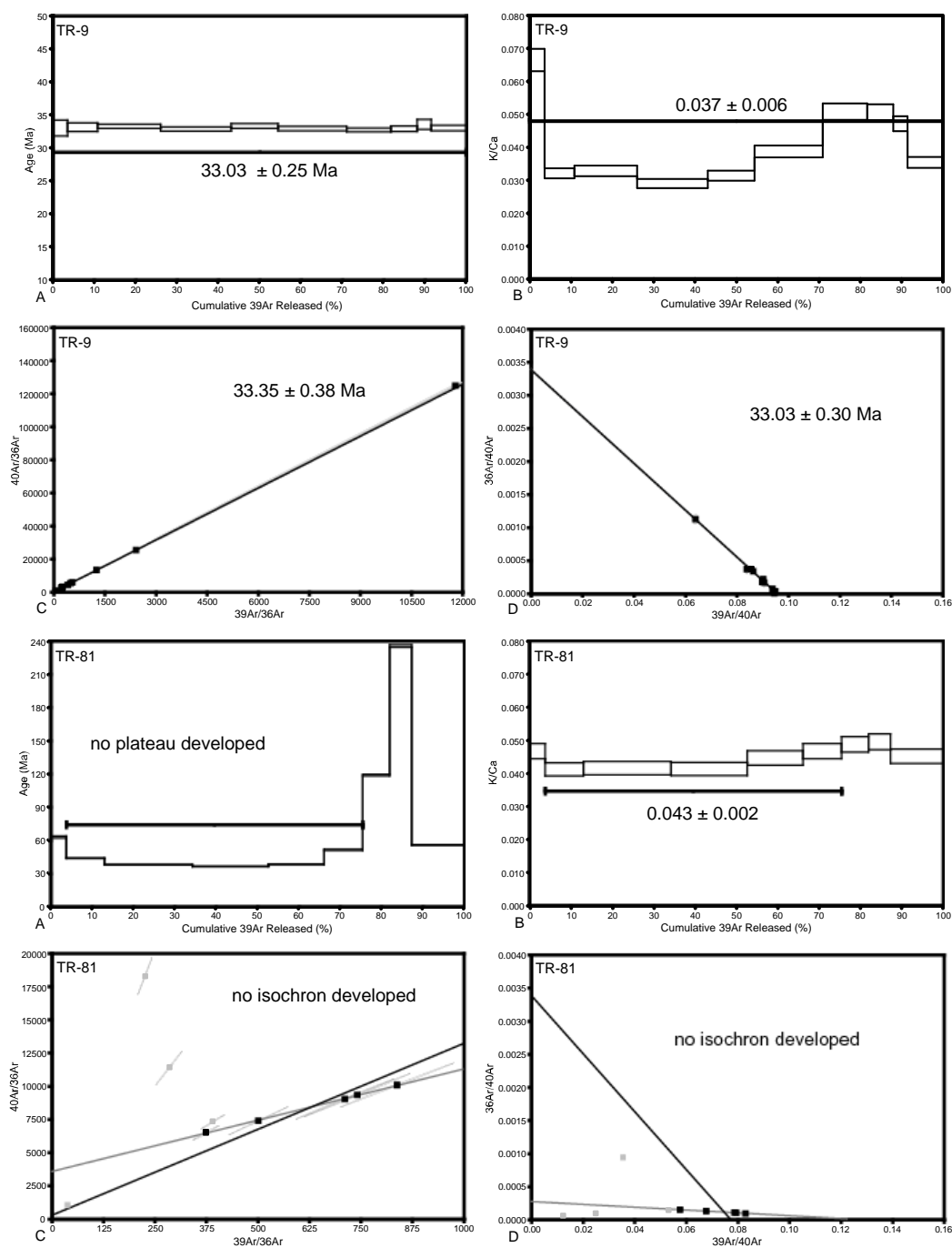


Figure 13. $^{40}\text{Ar}/^{39}\text{Ar}$ age data, A) weighted age plateau, B) K-Ca plateau, C) normal isochron plot, D) inverse isochron plot. Thick line seen in the plateau plots represents the heating steps used to determine the age or ratio. In the isochron and inverse isochron plots, the black points and lines represent the best-fit line and the data used to create this line. The gray points represent data not within error of the best-fit line and the gray line serves as a reference for the expected best-fit line. When overlapping, the reference line cannot be distinguished from the best-fit line.

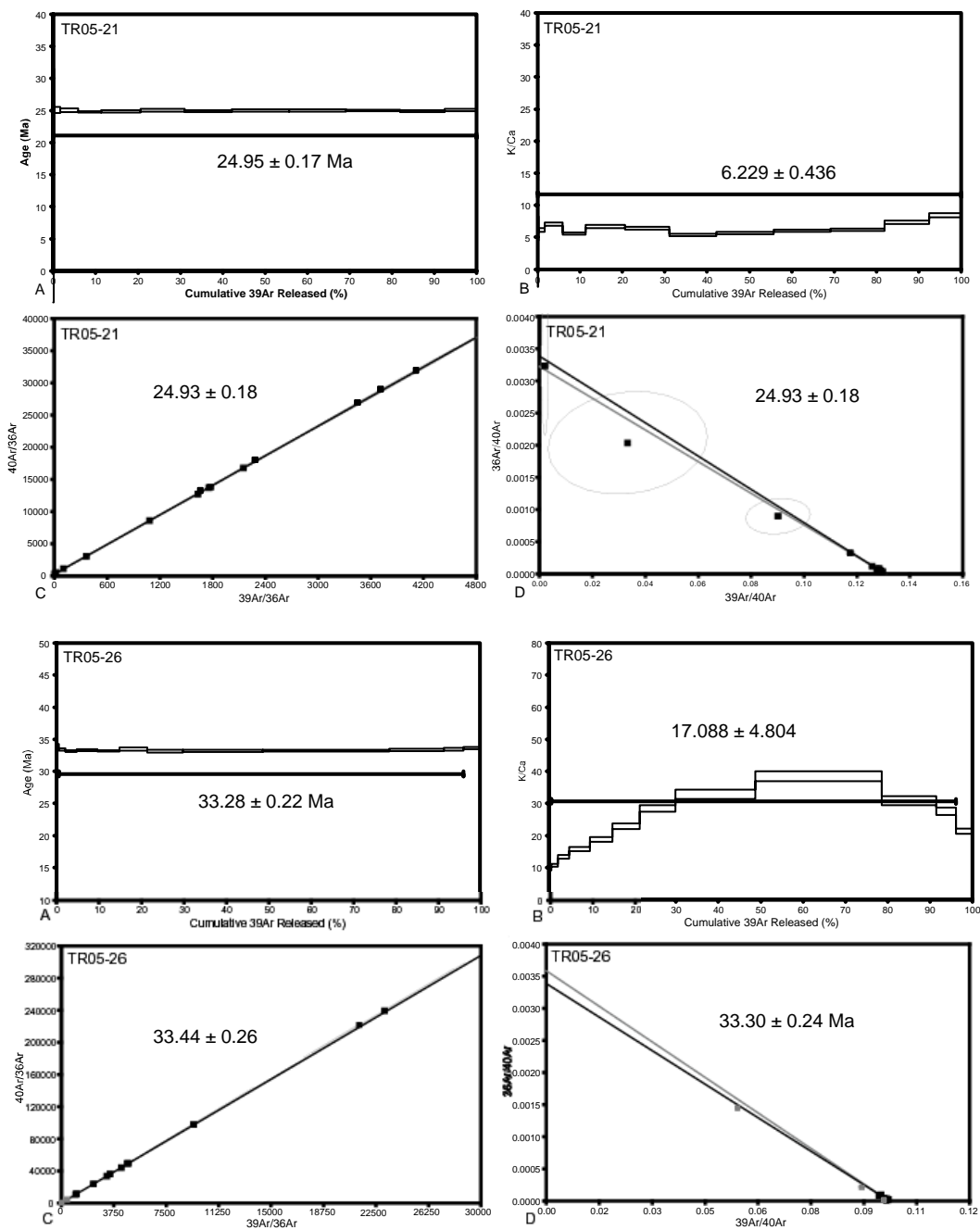


Figure 13. (cont.)

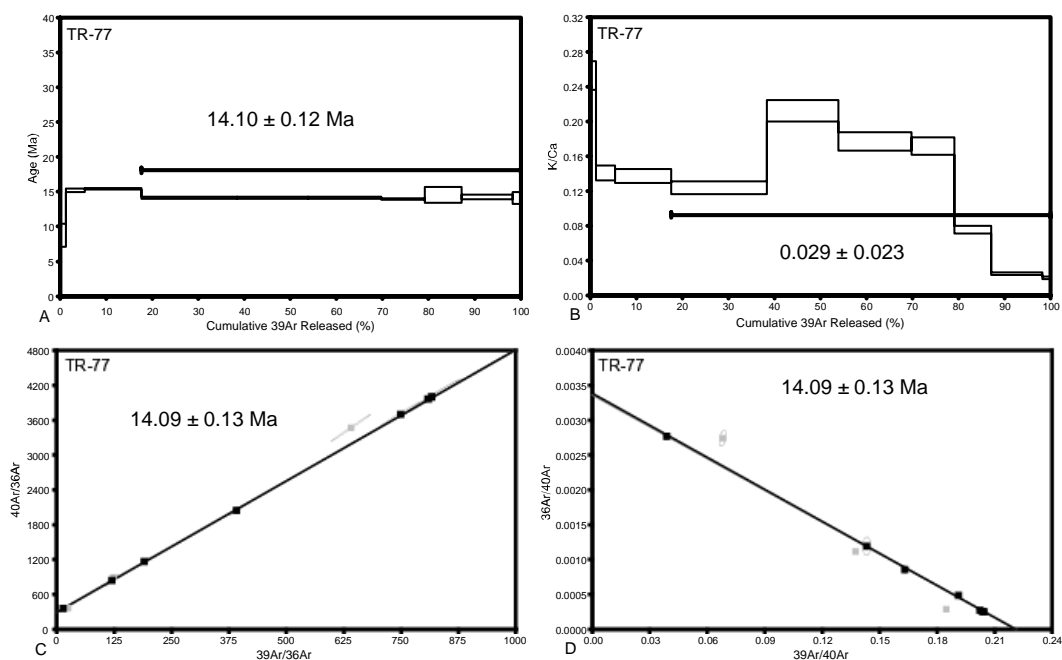


Figure 13. (cont.)

Geochemistry

Ten samples were submitted to ALS-Chemex for whole rock geochemical analysis. These samples were chosen to observe possible correlations between the various rhyolite ignimbrites found in Golconda Canyon. In addition, two andesite samples were analyzed, TR-9, an ignimbrite vitrophyre near the base of the andesite sequence which was radiometrically age dated, and TR-53, a lava flow near the top of the andesite sequence. Two analytical methods were used on the samples: method ME-MS61 analyzed for 47 trace elements with inductively coupled plasma mass spectroscopy (ICP-MS), and method ME-XRF06 determined oxide content for 13 elements and loss on ignition using x-ray fluorescence. Below are the detection limits for the respective methods (Table 3).

Table 3. Detection limits for the ICP-MS and x-ray fluorescence methods.

Method code	Description	Elements and Ranges (%)	
ME-XRF06	Whole rock analysis. All elements by lithium meta or tetra borate fusion* and XRF.	Si SiO ₂ (0.01 - 100)	Cr Cr ₂ O ₃ (0.01 - 100)
		Al Al ₂ O ₃ (0.01 - 100)	Ti TiO ₂ (0.01 - 100)
		Fe Fe ₂ O ₃ (0.01 - 100)	Mn MnO (0.01 - 100)
		Ca CaO (0.01 - 100)	P P ₂ O ₅ (0.01 - 100)
		Mg MgO (0.01 - 100)	Sr SrO (0.01 - 100)
		Na Na ₂ O (0.01 - 100)	Ba BaO (0.01 - 100)
		K K ₂ O (0.01 - 100)	Loss on Ignition (0.01 - 100)

Method code	47 elements by HF-HNO ₃ -HClO ₄ acid digestion, HCl leach and a combination of ICP-MS and ICP-AES.		
ME-MS61	Elements and Ranges (ppm)		
Ag (0.02 - 100)	Cu (0.2 - 10,000)	Na (0.01% - 10%)	Ta (0.05 - 100)
Al (0.01% - 25%)	Fe (0.01% - 25%)	Nb (0.1 - 500)	Te (0.05 - 500)
As (0.2 - 10,000)	Ga (0.05 - 500)	Ni (0.2 - 10,000)	Th (0.2 - 500)
Ba (0.5 - 10,000)	Ge (0.05 - 500)	P (10 - 10,000)	Ti (0.01% - 10%)
Be (0.05 - 1000)	Hf (0.1 - 500)	Pb (0.5 - 10,000)	Tl (0.02 - 500)
Bi (0.01 - 10,000)	In (0.005 - 500)	Rb (0.1 - 500)	U (0.1 - 500)
Ca (0.01% - 25%)	K (0.01% - 10%)	Re (0.002 - 50)	V (1 - 10,000)
Cd (0.02 - 500)	La (0.5 - 500)	S (0.01% - 10%)	W (0.1 - 10,000)
Ce (0.01 - 500)	Li (0.2 - 500)	Sb (0.05 - 1,000)	Y (0.1 - 500)
Co (0.1 - 10,000)	Mg (0.01% - 15%)	Se (1 - 1,000)	Zn (2 - 10,000)
Cr (1 - 10,000)	Mn (5 - 10,000)	Sn (0.2 - 500)	Zr (0.5 - 500)
Cs (0.05 - 500)	Mo (0.05 - 10,000)	Sr (0.2 - 10,000)	

Whole Rock Geochemistry Data

Below (Table 4) is data produced from the whole rock geochemistry analysis.

The map unit column correlates to the geologic units identified on the map. Tct – Caetano tuff, Trx – rhyolite landslide breccia, Tri – rhyolite ignimbrite, Trip – pumice-rich rhyolite ignimbrite, Trib – biotite-rich rhyolite ignimbrite, Tai – andesite ignimbrite, Tal – andesite lava. A digital version of the data is also available on the attached CD.

Table 4. Whole rock geochemistry data

Method ME-MS61 - ALS Chemex															
Element (ppm)	TR6 Tct	15 Tct	TR05-6 Tct	TR05-4 Tct	TR05-1 Trx	12 Tfe Trx	TR95 Trx	TR52 Tri	TR05-27 Trip	TR05-21 Trip	TOD 42 Trnb	TR05-26 Trib	TR9 Tai	TR53 Tal	
Ag	0.08	0.07	0.05	0.05	0.06	0.04	0.06	<0.01	0.1	0.27	0.08	0.13	0.08	0.08	
As	5.8	2.3	5.1	2.3	7.7	2.6	7.5	3.9	8.2	13.2	1.8	5	4.7	2.8	
Ba	560	1080	170	1480	460	310	400	290	700	590	1330	180	2570	1780	
Be	3.06	2.68	5.42	2.52	4.98	5.92	9.27	6.27	2.36	1.78	1.92	2.25	2.63	2.81	
Bi	0.13	0.08	0.29	0.14	0.1	0.08	0.04	0.07	0.02	0.07	0.02	0.16	0.1	0.01	
Cd	0.05	0.11	0.06	0.05	0.03	0.02	0.05	0.02	0.23	0.18	0.05	0.14	0.15	0.19	
Ce	76.2	102.5	38.2	108	192	148.5	123	110.5	81	88	100	46.3	86.8	97.5	
Co	1.3	1.4	1.1	1.4	1.4	0.8	1.1	1.2	1.1	0.7	1.4	3.9	6.7	9.7	
Cr	30	26	22	18	33	26	19	48	26	16	37	41	12	31	
Cs	1.72	1.7	8.09	2	3.68	6.16	4.15	1.98	4.64	4.18	2.02	25.8	41.6	2.01	
Cu	4	22.6	3.3	27.1	8.8	5.9	5.8	6.6	8.6	9.7	3.3	33.9	3.3	11.9	
Ga	19.45	19.25	19.5	19.5	23.5	25.5	28.2	22.8	21	18.35	18.65	17.25	24.8	21.5	
Ge	0.11	0.13	0.09	0.13	0.21	0.16	0.18	0.16	0.15	0.14	0.13	0.09	0.15	0.15	
Hf	3.6	3.7	3.6	3.8	4.7	7.3	10.6	6.7	5.1	5.6	2.6	2.8	8.7	5.4	
In	0.03	0.028	0.041	0.03	0.054	0.058	0.068	0.07	0.045	0.069	0.024	0.035	0.05	0.032	
La	39.1	56.6	18.1	59.6	109	69.9	58.1	64.6	38	44.5	54.3	19.9	41.5	54.4	
Li	28.6	18.6	19.7	31	31.8	45.4	52.6	89.1	13.8	25.3	12.7	13.9	16.2	39.1	
Mn	121	164	232	133	108	96	110	96	574	289	46	156	590	459	
Mo	0.96	1.97	0.93	0.85	4.02	1.16	0.8	0.81	2.73	0.57	0.73	0.31	2.46	2.27	
Nb	14.2	13	16.6	13	23.1	33.1	54.8	18.6	26	26.1	12.8	15.4	15.8	13.4	
Ni	1.4	1.1	1.5	0.8	1.7	1.1	1.2	2	3	1.3	1.2	6.1	1	5.9	
P	150	210	90	290	230	150	200	110	340	230	220	50	1470	1690	
Pb	27.2	22.3	29.2	20.5	24.7	26.8	39.5	25.3	32	137.5	26.5	57.3	17.6	16.4	
Rb	187	167.5	225	154.5	198.5	309	440	313	223	192.5	137.5	52.1	53.4	109.5	

Table 4. (continued)

Method ME-MS61 - ALS Chemex														
Element (ppm)	TR6 Tct	15 Tct	TR05-6 Tct	TR05-4 Tct	TR05-1 Trx	12 Tfe Trx	TR95 Trx	TR52 Tri	TR05-27 Trip	TR05-21 Trip	TOD 42 Trib	TR05-26 Trib	TR9 Tai	TR53 Tal
Re	<0.002	0.4	0.21	<0.002	<0.002	<0.002	<0.002	<0.002	0.004	0.003	0.002	0.002	<0.002	<0.002
Sb	0.4	0.21	0.31	0.26	0.85	5.91	1.4	0.95	1.48	3.33	0.31	1.08	0.59	0.29
Se	1	1	1	1	1	2	2	1	<1	1	<1	<1	1	1
Sn	2.5	2.4	3.8	2	2.6	5.1	8.3	5.5	0.8	2.9	1.6	3.2	2.3	1.1
Sr	146	233	351	277	84.2	46.8	92.8	76	109.5	77.7	247	258	1440	1005
Ta	1.18	0.98	1.84	0.91	1.64	2.95	5.3	2.53	1.68	1.72	0.84	1.55	1.06	0.82
Te	<0.05	<0.05	<0.05	<0.05	<0.05	<0.05	<0.05	<0.05	<0.05	<0.05	<0.05	<0.05	<0.05	<0.05
Th	23.4	22.2	25.7	20.7	31.9	41.8	53.8	32.9	19	21.4	20	22.1	17.4	11.7
Tl	0.97	0.84	1.24	0.73	1	1.33	2.31	1.81	1.01	1.45	0.76	0.61	1.01	0.34
U	3.7	3.2	4.9	2.8	5.7	7.8	12.4	6	6.7	5	3.5	4	4.4	2.6
V	7	8	8	8	15	6	17	9	10	10	9	14	113	91
W	1.1	1.1	1.2	1.3	2.8	1.1	1.6	0.7	3.3	16.7	1.2	0.8	1.5	1.1
Y	19.2	16.9	22.6	15.4	39.5	43.6	62.3	40.3	24.3	30.3	14.3	16	25	27
Zn	40	37	44	35	49	60	96	45	72	47	42	132	78	78
Zr	80	86.5	70	94.7	104.5	133.5	181	142.5	189	190	68.7	65.1	273	167.5

Method ME-MS61 - ALS Chemex														
Element (%)	TR6 Tct	15 Tct	TR05-6 Tct	TR05-4 Tct	TR05-1 Trx	12 Tfe Trx	TR95 Trx	TR52 Tri	TR05-27 Trip	TR05-21 Trip	TOD 42 Trib	TR05-26 Trib	TR9 Tai	TR53 Tal
Al	7.34	7.48	6.87	7.81	6.81	6.63	7.08	6.19	6.3	6.03	7.27	6.75	9.57	8.16
Ca	0.88	1	1.19	1.25	0.91	0.38	0.41	0.99	1.36	0.99	0.91	1.06	4.4	2.79
Fe	1.2	1.26	0.93	1.35	1.68	1.18	1.25	0.92	1.55	1.36	1.26	0.96	3.17	3.35
K	4.74	4.66	3.83	4.46	4.55	4.4	5.24	4.87	5.17	4.23	4.1	1.14	1.1	3.06
Mg	0.16	0.26	0.26	0.24	0.06	0.05	0.13	0.1	0.19	0.08	0.15	0.41	1.04	0.84
Na	2.19	1.98	1.42	1.94	2.3	2.23	2.38	1.82	1.88	1.97	1.63	1	2.37	2.85
S	<0.01	0.03	0.02	0.03	<0.01	<0.01	0.01	0.06	0.01	0.01	<0.01	0.02	0.01	0.05
Ti	0.079	0.109	0.045	0.14	0.118	0.075	0.103	0.068	0.135	0.114	0.106	0.064	0.505	0.37

Table 4. (continued)

Method ME-XRF06 - ALS Chemex															
Oxide (%)	TR6 Tct	15 Tct	TR05-6 Tct	TR05-4 Tct	TR05-1 Trx	12 Tfe Trx	TR95 Trx	TR52 Tri	TR05-27 Trip	TR05-21 Trip	TOD 42 Trib	TR05-26 Trib	TR9 Tai	TR53 Tai	
SiO2	72.55	71.25	71.37	69.64	71.84	74.15	71.86	75.09	67.62	71.7	70.28	69.41	56.83	63.79	
Al2O3	13.89	14.34	13.01	14.82	13.37	13.22	13.86	11.65	13.09	12.61	14.46	13.26	18.18	15.05	
Fe2O3	1.64	1.74	1.35	1.87	2.37	1.74	1.77	1.3	2.31	2.07	1.79	1.38	4.39	5.1	
CaO	1.22	1.35	1.66	1.68	1.31	0.54	0.55	1.34	1.92	1.46	1.26	1.53	5.58	3.95	
MgO	0.31	0.43	0.43	0.39	0.1	0.06	0.19	0.11	0.36	0.15	0.28	0.74	1.8	1.47	
Na2O	3.07	2.86	2.17	2.74	3.26	3.31	3.38	2.55	2.87	3.3	2.4	1.52	3.44	3.9	
K2O	5.38	5.31	4.37	5.06	5.62	5.89	6.26	5.44	6.72	5.58	5.09	1.45	1.15	3.27	
Cr2O3	0.01	<0.01	<0.01	<0.01	<0.01	<0.01	0.01	0.01	<0.01	<0.01	<0.01	<0.01	<0.01	<0.01	
TiO2	0.21	0.24	0.11	0.25	0.25	0.2	0.26	0.14	0.26	0.22	0.19	0.08	0.84	0.69	
MnO	0.01	0.02	0.02	0.01	0.01	0.01	0.01	0.01	0.07	0.03	<0.01	0.01	0.06	0.06	
P2O5	0.02	0.05	0.03	0.08	0.05	0.03	0.05	0.02	0.08	0.06	0.05	0.02	0.31	0.35	
SrO	0.02	0.03	0.05	0.04	0.01	0.01	0.02	0.01	0.01	0.01	0.03	0.03	0.17	0.12	
BaO	0.06	0.12	0.03	0.14	0.06	0.03	0.05	0.03	0.08	0.07	0.15	0.02	0.25	0.19	
LOI	1.44	2.24	5.14	2.94	1.33	0.66	1.62	2.15	2.92	1.99	2.63	8.99	6.84	2.02	
Total	99.84	99.97	99.74	99.68	99.59	99.85	99.88	99.86	98.32	99.25	98.61	98.45	99.83	99.95	

GIS Database

A GIS database of the geologic map created for this research is on the accompanying CD. This database consists of a number of shapefiles containing the data collected for completion of the geologic map. Previous geologic mapping of this area consists of the 1:250,000-scale Geologic Map of Pershing County (Tatlock et al., 1977) and a 1:24,000-scale geologic map by Burke (1973) which extends from Golconda Canyon southward to the termination of the Tobin Range. Map data was collected in the field using 1:12,000-scale air photos and topographic maps and later redrafted in ESRI ArcGIS 9 using digital orthophotos and 7.5-minute topographic maps as base maps. Drafting of the map was completed as a digital database to allow for increased accessibility and for the ability to easily integrate this data with other digital data. The database was created for use at a scale of 1:24,000. A final version of the geologic map is also provided as a .pdf for reference (digital version of Plate 1).